cmgh
CELLULAR AND MOLECULAR GASTROENTEROLOGY AND HEPATOLOGY

ORIGINAL RESEARCH

The Histamine Pathway is a Target to Treat Hepatic Experimental Erythropoietic Protoporphyria

Ning Kuo,[1,4] Pei Li,[1] Juliana Bragazzi Cunha,[1,5] Lu Chen,[1] Jordan A. Shavit,[2,3] and M. Bishr Omary[1]

[1]Robert Wood Johnson Medical School, and Center for Advanced Biotechnology and Medicine, Rutgers University, Piscataway, New Jersey; [2]Department of Pediatrics, Division of Pediatric Hematology/Oncology, University of Michigan, Ann Arbor, Michigan; [3]Department of Human Genetics, University of Michigan, Ann Arbor, Michigan; [4]Current affiliation: Biomedical Sciences Graduate Program, University of California San Diego, La Jolla, California; and [5]Current affiliation: Division of Hospital Medicine, Department of Internal Medicine, University of Michigan, Ann Arbor, Michigan

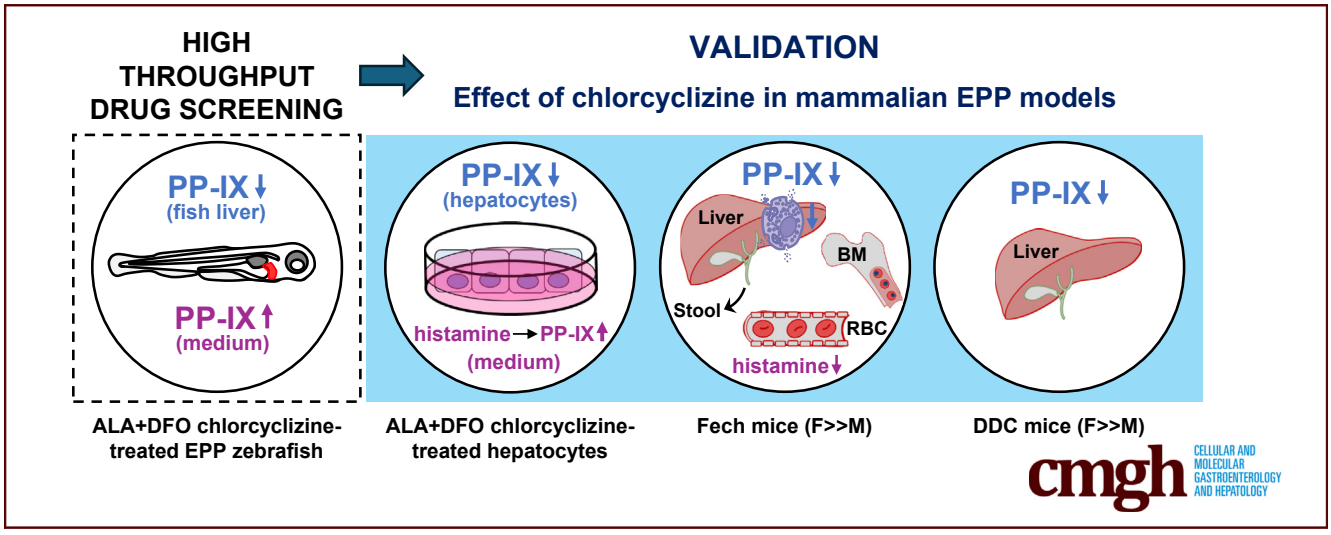

SUMMARY

Liver transplantation is the primary treatment for end-stage liver disease due to erythropoietic protoporphyria and consequent protoporphyrin-IX accumulation. We show that chlorcyclizine and other antihistamines lower hepatocyte and bone marrow protoporphyrin-IX levels and, therefore, may serve as effective therapeutic alternatives.

BACKGROUND & AIMS: Erythropoietic protoporphyria (EPP) is caused by mutations in ferrochelatase, which inserts iron into protoporphyrin-IX (PP-IX) to generate heme. EPP is characterized by PP-IX accumulation, skin photosensitivity, cholestasis, and end-stage liver disease. Despite available drugs that address photosensitivity, treatment of EPP-related liver disease remains an unmet need.

METHODS: We administered delta-aminolevulinic acid (ALA) and deferoxamine (DFO), which results in PP-IX overproduction and accumulation. High-throughput compound screening of ALA + DFO-treated zebrafish identified chlorcyclizine (first generation H1-antihistamine receptor blocker) as a drug that reduces zebrafish liver PP-IX levels. The effect of chlorcyclizine was validated in porphyrin-loaded primary mouse hepatocytes (PMHs), transgenic Fech^{m1Pas} EPP mice, and mice fed the porphyrinogenic compound 3,5-diethoxycarbonyl-1,4-dihydrocollidine (DDC). Plasma and tissue PP-IX were measured by fluorescence; livers were analyzed by histology, immunoblotting, and quantitative polymerase chain reaction.

RESULTS: Chlorcyclizine-treated zebrafish larvae, DDC-fed, and transgenic EPP mice manifested reduced hepatic PP-IX levels compared with controls. Histamine increased PP-IX accumulation in porphyrin-stressed hepatocytes, whereas H1/H2-receptor blockade decreased PP-IX levels. In both mouse models, chlorcyclizine lowered PP-IX levels in female but not male mice in liver, erythrocytes, and bone marrow; improved liver injury; decreased porphyrin-triggered protein aggregation and oxidation; and increased clearance of stool PP-IX. In PMHs, chlorcyclizine induced nuclear translocation of constitutive androstane and farnesoid X receptors, and transactivated bile acid transporter expression. Knockdown of the transporters BSEP and MRP4 led to increased detection of sequestosome-1 (p62 protein) high-molecular-weight species. Chlorcyclizine also reduced hepatic mast cell number and histamine level in EPP mice.

CONCLUSIONS: Histamine plays an important role in PP-IX accumulation in zebrafish and 2 experimental EPP models. Chlorcyclizine and/or other antihistamines provide a potential therapeutic strategy to treat EPP-associated liver disease via

decreasing PP-IX accumulation. *(Cell Mol Gastroenterol Hepatol 2025;19:101463; https://doi.org/10.1016/j.jcmgh.2025.101463)*

Keywords: Anti-H1 Histamine Blocker; Anti-H2 Histamine Blocker; Ferrochelatase; Porphyria-related Liver Disease.

This article has an accompanying editorial.

Erythropoietic protoporphyria (EPP, OMIM: 177000) is caused by the loss of ferrochelatase activity below 30% of normal, leading to accumulation of protoporphyrin-IX (PP-IX) in the liver and in bone marrow erythroid precursors.[1–3] Skin photosensitivity is a major manifestation of EPP,[3] and 10% to 25% of patients with EPP develop liver dysfunction and gallstones,[1,3] with 1% to 4% of overall cases progressing to end-stage liver failure needing transplantation.[4,5] Despite availability of drugs that relieve skin symptoms,[6,7] a mechanism-based therapeutic for EPP-related liver disease remains an unmet need.

Using our previously described zebrafish EPP model,[8] we screened 2560 approved and bioactive compounds in the Prestwick Chemical Library and the Library of Pharmaceutically Active Compounds (LOPAC) and identified the histamine receptor type 1 (H1)-antihistamine chlorcyclizine (CCZ) as a potent PP-IX lowering agent. In mice, EPP can be modeled genetically by the homozygous Fech^{m1Pas} (fch/fch) mice[9] or pharmacologically by feeding mice with a diet containing 3,5-diethoxycarbonyl-1,4-dihydrocollidine (DDC).[10] In fch/fch and DDC-fed mice, CCZ exerted a dramatic female-selective effect of clearing PP-IX. CCZ led to nuclear translocation of the constitutive androstane and farnesoid X receptors from the cytoplasm, driving transcription of the multidrug resistance-associated protein-4 (MRP4) and bile salt export pump (BSEP) and increased PP-IX excretion. In primary mouse hepatocyte (PMH) cultures, CCZ also inhibited the stimulatory effect of histamine on porphyrin synthesis and reduced PP-IX mediated protein aggregation.

The involvement of the histamine pathway in EPP led us to further investigate the potential role of mast cells (MCs), whose increased presence has been implicated in several liver diseases.[11,12] In fch/fch mice, we observed elevated plasma and hepatic histamine levels with liver mast cell infiltrates. Notably, CCZ administration reduced hepatic MC number and histamine level. Taken together, histamine inhibition, as demonstrated by CCZ and other antihistamines, represents a unique therapeutic strategy to repurpose for treating EPP-associated liver disease.

Results

Quantitative High-throughput Drug Screening Led to the Identification of CCZ as a Porphyrin-lowering Agent

An unbiased, quantitative high-throughput drug screening (qHTS) of the Prestwick Chemical Library and the LOPAC was carried out using a precursor-induced zebrafish EPP model that we previously established[8] (Figure 1). In this model, overproduction of endogenous PP-IX was induced by retro-orbital injection of the heme precursor δ-aminolevulinic acid hydrochloride (ALA) and the iron chelator deferoxamine mesylate (DFO) into zebrafish A3 larvae. When compared with water-injected control (Figure 2*A*, *panel a*), co-administration of ALA and DFO resulted in elevated PP-IX synthesis and subsequent accumulation in the liver and biliary system (Figure 2*A*, *panels a, b*). Of the 2560 compounds that were screened, the H1-antihistamine CCZ was selected for further study, based on consistent robust reduction in hepatic PP-IX levels. When evaluated at higher doses, CCZ led to greater decrease in hepatic PP-IX accumulation (Figure 2*A, B*), and a 2.6-fold increase in excreted PP-IX level in the fish growth medium (Figure 2*C*). We then validated the initial drug screen result in cultured PMHs treated with ALA + DFO and measured PP-IX fluorescence in the cell lysates and medium (Figure 2*D*). In support of the primary screen result in zebrafish, CCZ similarly decreased intracellular PP-IX level in a dose-dependent manner. There was no significant change in medium PP-IX level following 12 hours of CCZ treatment.

CCZ Induces PP-IX Clearance and Reduces Liver Injury in Female fch/fch Mice

Fech^{m1Pas} (fch/fch) mice were previously reported to closely phenocopy the more severe forms of human EPP.[9] As expected, fch/fch mice display hepatomegaly with a liver-to-body weight ratio nearly double the ratio in wild-type mice (Figure 2*E*). In the fch/fch livers, particulate PP-IX deposits were found to accumulate mostly in the bile canaliculi and interlobular ducts (Figure 2*F*, *panel a, b*). The extent of hepatic PP-IX accumulation was assessed by the percent area (Figure 2*F*) and total counts (Figure 2*G*) of the dark brown PP-IX deposits. Consistent with what we observed in zebrafish and cultured PMHs, administration of CCZ (25 mg/kg) led to significant reduction in the hepatic PP-IX area and counts in female, but not male, mice. To further analyze the histologic profile of the hepatic PP-IX deposits, we

Abbreviations used in this paper: **ALA, δ-aminolevulinic acid; ALP, alkaline phosphatase; ALT, alanine aminotransferase; ANOVA, analysis of variance; BSEP, bile salt export pump; CAR, constitutive androstane receptor; CCZ, chlorcyclizine; CMT, cimetidine; DDC, 3,5-diethoxycarbonyl-1,4-dihydrocollidine; DFO, deferoxamine mesylate; DMSO, dimethyl sulfoxide; EPP, erythropoietic protoporphyria; fch/fch, Fech^{m1Pas}; FITC, fluorescein isothiocyanate; FXR, farnesoid-X receptor; H1, H2, histamine receptor types 1 and 2; HRH1, histamine receptor type 1; HMW, high molecular weight; LOPAC, Library of Pharmaceutically Active Compounds; MC, mast cell; MCP1, mast cell protease-1; MRP4, multidrug resistance-associated protein 4; PMH, primary mouse hepatocytes; PP-IX, protoporphyrin IX; qHTS, quantitative high-throughput drug screening; qRT-PCR, quantitative real-time polymerase chain reaction; ROS, reactive oxygen species; RXR, retinoid X receptor; SD, standard deviation; siRNA, small interfering RNA; XLP, X-linked protoporphyria.**

Most current article

2352-345X
https://doi.org/10.1016/j.jcmgh.2025.101463

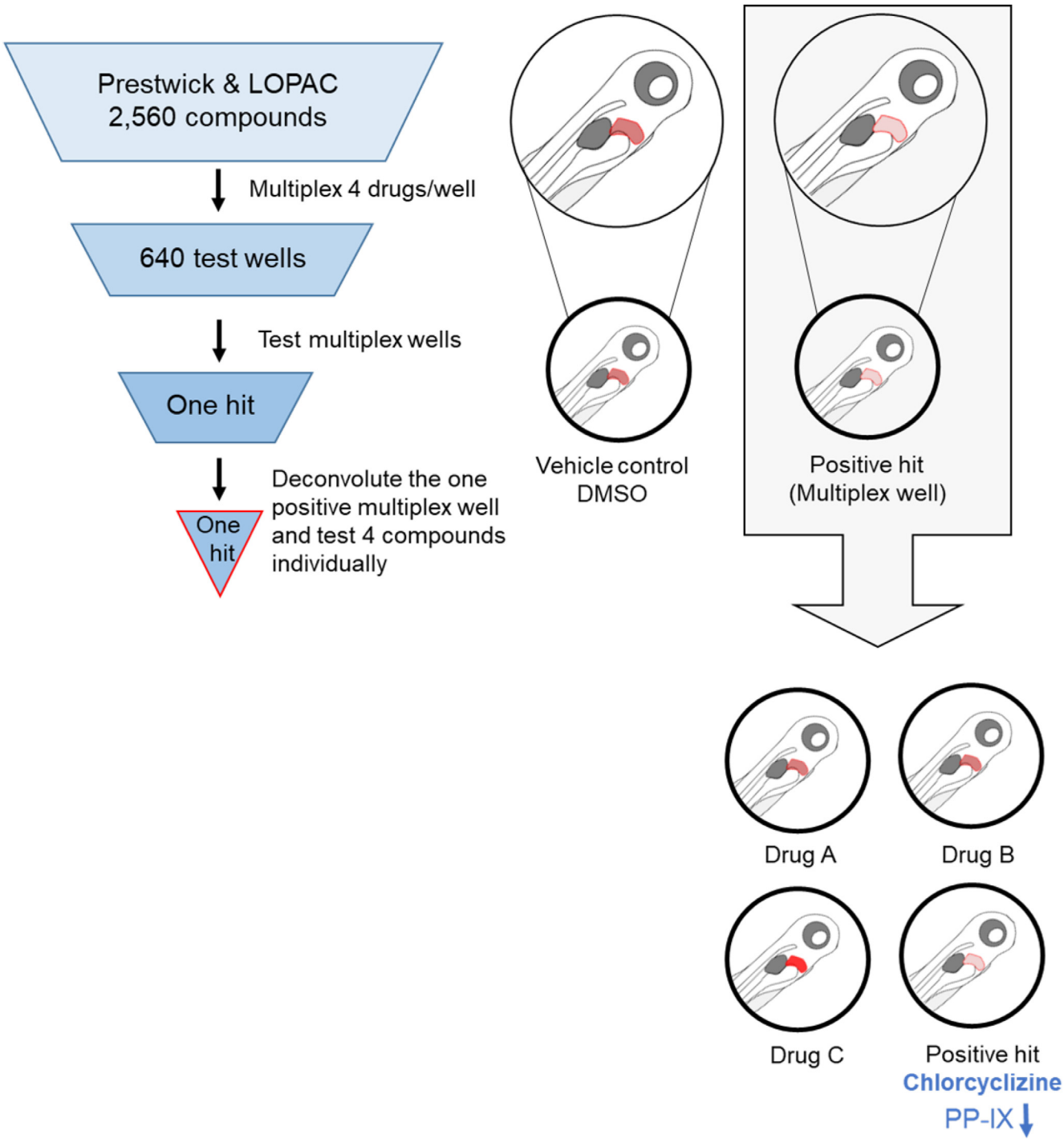

Figure 1. Schematic of the high-throughput drug screening in experimental EPP zebrafish. A total of 2560 compounds were multiplexed into 640 test wells. Positive hits were identified on the basis of significant reduction of the PP-IX (*red*) signal in EPP zebrafish livers (n ≥10 fish larvae; N ≥4 experiments). Funnel cartoons represent the progressive flow in the number of active compounds toward a validated optimal hit/compound for further investigation. Note the decrease in red liver fluorescence (right upper part of the schematic).

sorted each PP-IX deposit into 3 different size categories: small (0–25 μm^2), medium (>25–75 μm^2), and large (>75 μm^2). Our analysis revealed that the PP-IX deposits most reduced in female livers were primarily medium-sized deposits (Figure 2*H*).

To determine whether CCZ changes porphyrin levels in tissues aside from the liver, we measured PP-IX in known target tissues such as the liver, erythrocytes (inclusive of leukocytes), bone marrow, and plasma, as well as key routes that PP-IX takes to exit the body, which are the bile and

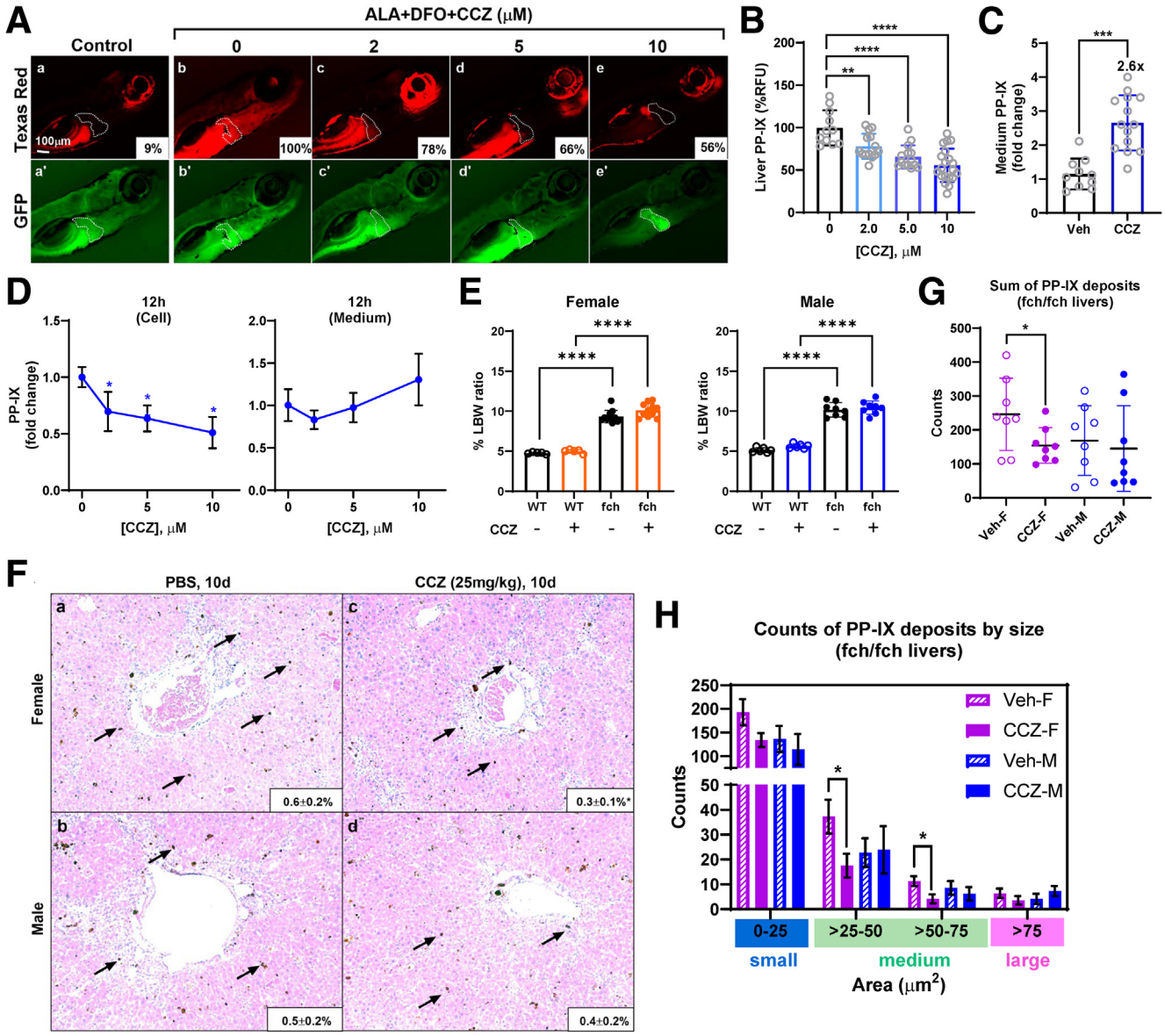

Figure 2. CCZ reduces PP-IX accumulation in experimental zebrafish, PMH, and fch/fch mouse EPP models. (*A*) Representative fluorescence images of EPP zebrafish larvae treated with the vehicle DMSO and CCZ at indicated concentrations. (*B*) Quantification of zebrafish liver PP-IX fluorescence as mean ± SD (9 ± 4%, 100 ± 20%, 78 ± 15%, 66 ± 14%, 56 ± 20%). (*C*) PP-IX levels in the zebrafish culture medium normalized to the level in the DMSO-treated controls (n ≥10 larvae per condition, N = 4 experiments). (*D*) Freshly isolated hepatocytes from FVB/N mice were treated with vehicle or ALA + DFO for 12 hours. Relative PP-IX fluorescence in the hepatocytes and culture medium is shown normalized to the level in the untreated ALA + DFO group. Data are shown as mean ± SD (N = 4 experiments). (*E*) fch/fch mice manifest increased % liver-to-body weight (LBW) ratio that is nearly double the ratio of wild-type (WT) mice (female fch: 9.3 ± 0.8%; female WT: 4.8 ± 0.1%; male fch: 10 ± 0.9%; male WT: 5.1 ± 0.3%). CCZ does not alter the LBW ratio. Data are shown as mean ± SD (n = 5–8 mice per group, N = 2 experiments). Statistical analysis was performed using the 1-way ANOVA test, ****$P < .0001$. (*F*) fch/fch male and female mice were treated with PBS or CCZ. Representative H&E liver sections and quantification of PP-IX area in the male and female fch/fch mice is shown. *Arrows* indicate medium-sized PP-IX deposits (n = 8 mice per group, N = 2 experiments). (*G*) Quantification of total PP-IX counts in male (M) and female (F) fch/fch livers treated with vehicle (Veh/PBS) or CCZ. (*H*) Quantification of small-, medium-, and large-sized PP-IX deposits. Data are shown as mean ± SD (n = 8 mice/group, N = 2 experiments). For panels (*B–D*) and (*F–H*) statistical analysis was performed by 2-tailed Student *t*-test. ****$P < .0001$; ***$P < .001$; **$P < .01$; *$P < .05$.

stool.[9,13] Notably, in female but not male mice, CCZ reduced PP-IX levels in the liver, erythrocytes, and bone marrow, while increasing PP-IX excretion into stool (Figure 3*A*). There was no significant changes in plasma and bile PP-IX levels (Figure 3*A*). CCZ treatment also led to a decrease in the plasma liver injury markers alanine aminotransferase (ALT), alkaline phosphatase (ALP), and total bilirubin (Figure 3*B*). Total stool PP-IX output during the entire 10-

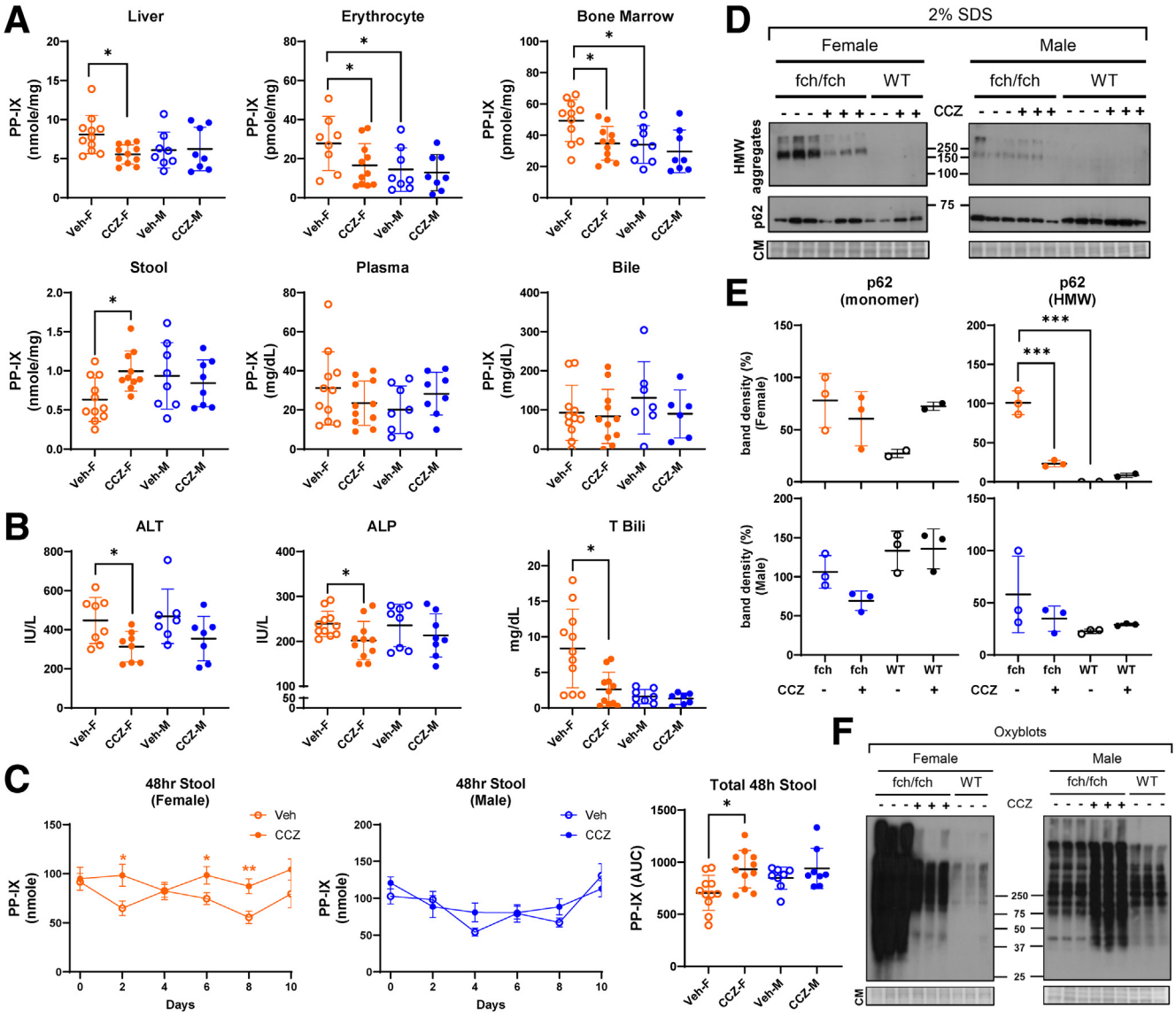

Figure 3. CCZ reduces tissue PP-IX levels and liver injury and protein oxidation in female but not male fch/fch mice. (*A*) PP-IX levels in the liver, erythrocytes, bone marrow, internal rectal stool, plasma, and bile. (*B*) Plasma ALT, ALP, and total bilirubin levels. (*C*) Cage stool was collected every 48 hours. Stool PP-IX levels were then measured. Total stool PP-IX level over the 10-day study period was calculated using the integrated area under the fluorescence curve. Data are shown as mean ± SD (n = 8–11 mice/group, N = 2 experiments). Statistical analysis was performed by ANOVA test, $^{*}P < .05$. (*D*) Immunoblots of p62 monomer and its high molecular weight aggregates in 2% SDS-containing buffer. (*E*) Densitometry analysis of p62 monomer and high molecular weight aggregates. Statistical analysis was performed by 2-tailed Student *t*-test, $^{***}P < .001$. (*F*) Oxyblots of total fch/fch or wild-type livers treated with the vehicle PBS or CCZ. CM, Coomassie staining.

day study period increased in CCZ-treated females when compared with their vehicle-treated control (Figure 3*C*). Taken together, our data suggest CCZ treatment for as short as 10 days is sufficient to drive clearance of PP-IX from several target tissues into the stool, coupled with amelioration of liver injury and PP-IX deposition.

CCZ Reduces Porphyrin-mediated Protein Aggregation in Female fch/fch Liver

Accumulation of PP-IX leads to organelle-selective protein aggregation, thereby causing hepatocellular damage.[14,15] One previously identified protein prone to prominent aggregation upon porphyrinogenic stress is p62/sequestosome-1 (SQSTM1),[14] an adaptor protein involved in the ubiquitin-proteasome machinery. In fch/fch total liver extracts, p62 forms high molecular weight (HMW) aggregates that are resistant to dissociation in 2% SDS-containing buffer (Figure 3*D*). CCZ treatment reduced p62 aggregation in female but not male livers (Figure 3*D, E*). When assessed by immunofluorescence staining, the p62 signal was mostly diffuse, except for a handful of puncta that were scattered throughout the liver section (Figure 4). Consistent with the immunoblot findings, the overall p62 signal decreased dramatically in the CCZ-treated female but not male livers (Figure 4).

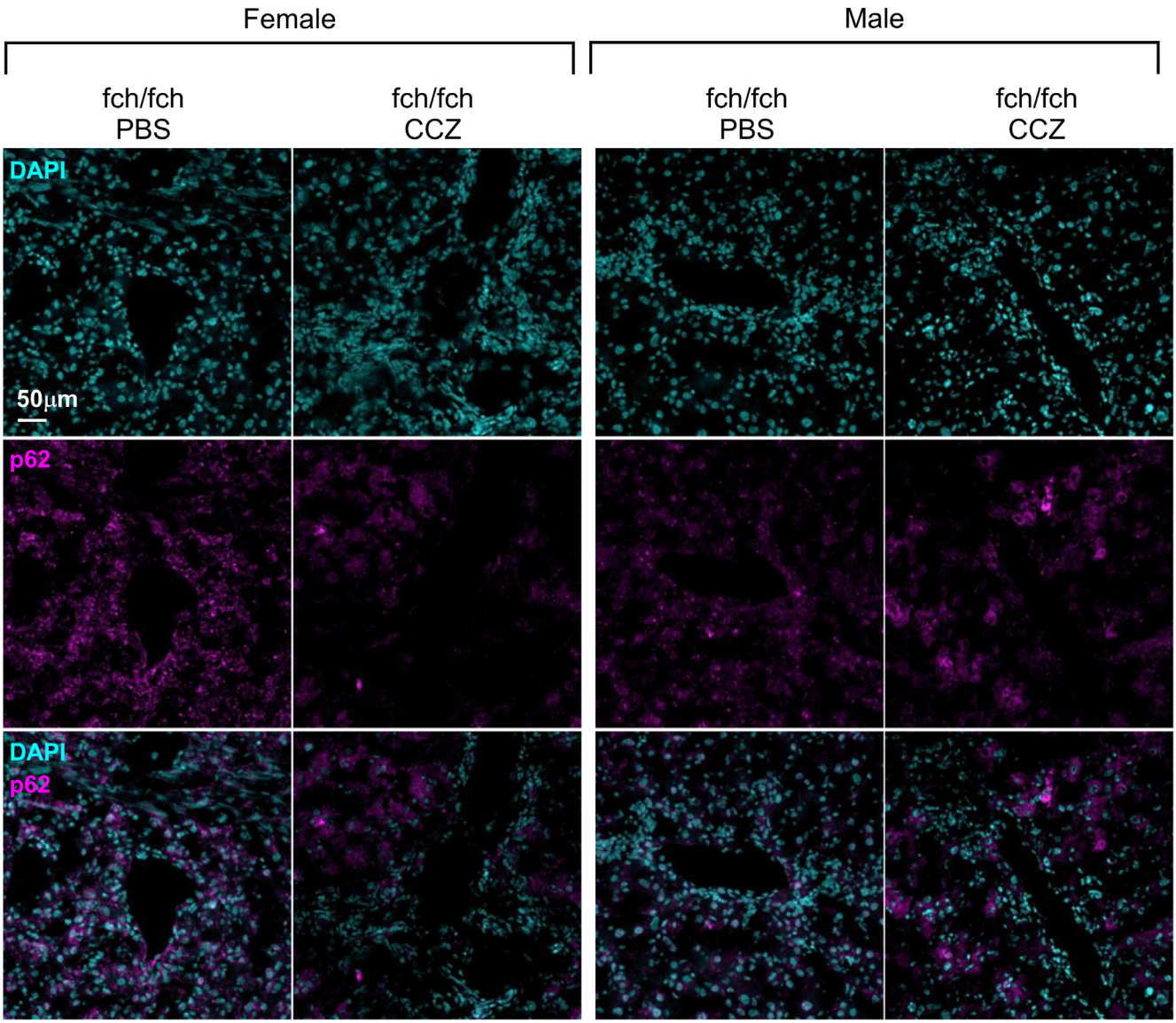

Figure 4. p62 immune staining of liver sections from fch/fch mice treated with vehicle (PBS) or CCZ. Representative images of liver sections isolated from female and male fch/fch mice, that were administered PBS or CCZ, were stained with DAPI (to label nuclei) and anti-p62 antibody. Female but not male livers showed reduced p62 staining (displayed in *pink*).

To globally assess the status of protein oxidation, we performed a protein carbonyl assessment of wild-type and fch/fch liver lysates. The oxyblots revealed that, compared with wild-type livers, fch/fch livers bore a much greater oxidative burden, likely due to the chronic porphyrinogenic stress (Figure 3*F*). Notably, although CCZ markedly reduced overall protein oxidation in female livers, it had no significant effect in male livers (Figure 3*F*).

CCZ Reduces PP-IX Level and Injury in Female DDC Liver

Some aspects of EPP can also be modeled by feeding mice with DDC, whose metabolite N-methyl PP-IX inhibits ferrochelatase.[10,14] Females were known to generate more PP-IX than males because they express higher levels of CYP3A1, which converts DDC into N-methyl PP-IX.[10,14] Similarly, in our case, after 5 days of DDC feeding, all mice had enlarged livers (Figure 5*A*), but a greater hepatic PP-IX area and counts in addition to excreted PP-IX in stool was seen in females than males (Figure 5*B, C*). Importantly, CCZ treatment led to significant reduction in PP-IX level in the female but not male livers (Figure 5*C*). Similar to female fch/fch liver, the PP-IX deposits most reduced by CCZ were within the medium-size >25 to 50 μm^2 range (Figure 5*D, E*). CCZ treatment did not cause significant changes in plasma ALT or ALP levels in DDC-fed female mice but increased plasma ALT levels in DDC-fed male mice (Figure 5*F*), possibly due to hepatotoxic drug-drug interaction between DDC, CCZ, and their metabolites.

Histamine is Porphyrinogenic and can be Blocked by H1 and H2 Antihistamines

To determine whether CCZ acts through the histamine receptor signaling pathway, we performed a dose-response

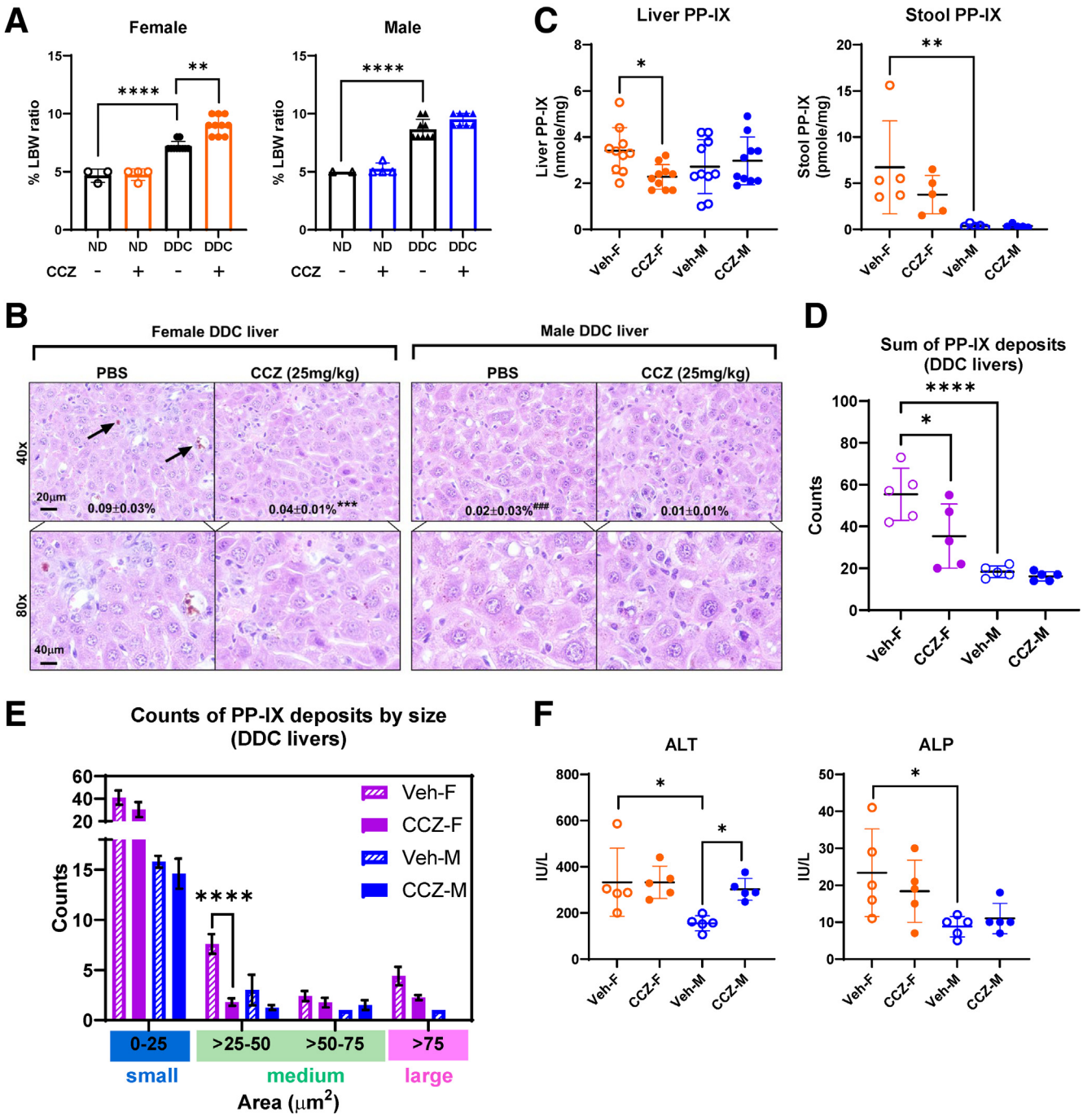

Figure 5. Effect of CCZ on PP-IX levels and liver injury in DDC-fed mice. (*A*) Prominent liver-to-body weight ratio (LBW) was observed in mice fed with DDC-containing diet for 5 days (female DDC: 7.2 ± 0.4%; female normal diet [ND]: 4.7 ± 0.6%; male DDC: 8.7 ± 0.9%; male ND: 5.0 ± 0.1%). CCZ further increases the liver-to-body weight ratio in the DDC-fed female mice (female DDC + CCZ: 9.0 ± 0.8%). Data are shown as mean ± SD (n = 2–10 mice per group, N = 2). Statistical analysis was performed using the 1-way ANOVA test. ****$P < .0001$; **$P < .01$. (*B*) Representative H&E liver sections and quantification of PP-IX deposit area in the livers of DDC-fed mice treated with PBS or CCZ. *Arrows* indicate PP-IX deposits. *** ($P < .001$) when comparing PBS with CCZ in females; ### ($P < .001$) when comparing PBS with CCZ in male mice. (*C*) PP-IX levels in the liver and stool isolated from the rectum. (*D*) Quantification of total PP-IX deposits in livers isolated from DDC-fed (5 days) mice. (*E*) Quantification of small-, medium-, and large-sized PP-IX deposits in the livers of DDC-fed mice. (*F*) Plasma ALT and ALP levels. Data are shown as mean ± SD (n = 5–10 mice per group, N = 2). Statistical analysis was performed using the 1-way ANOVA test. ****$P < .0001$; ***$P < .001$; **$P < .01$; *$P < .05$.

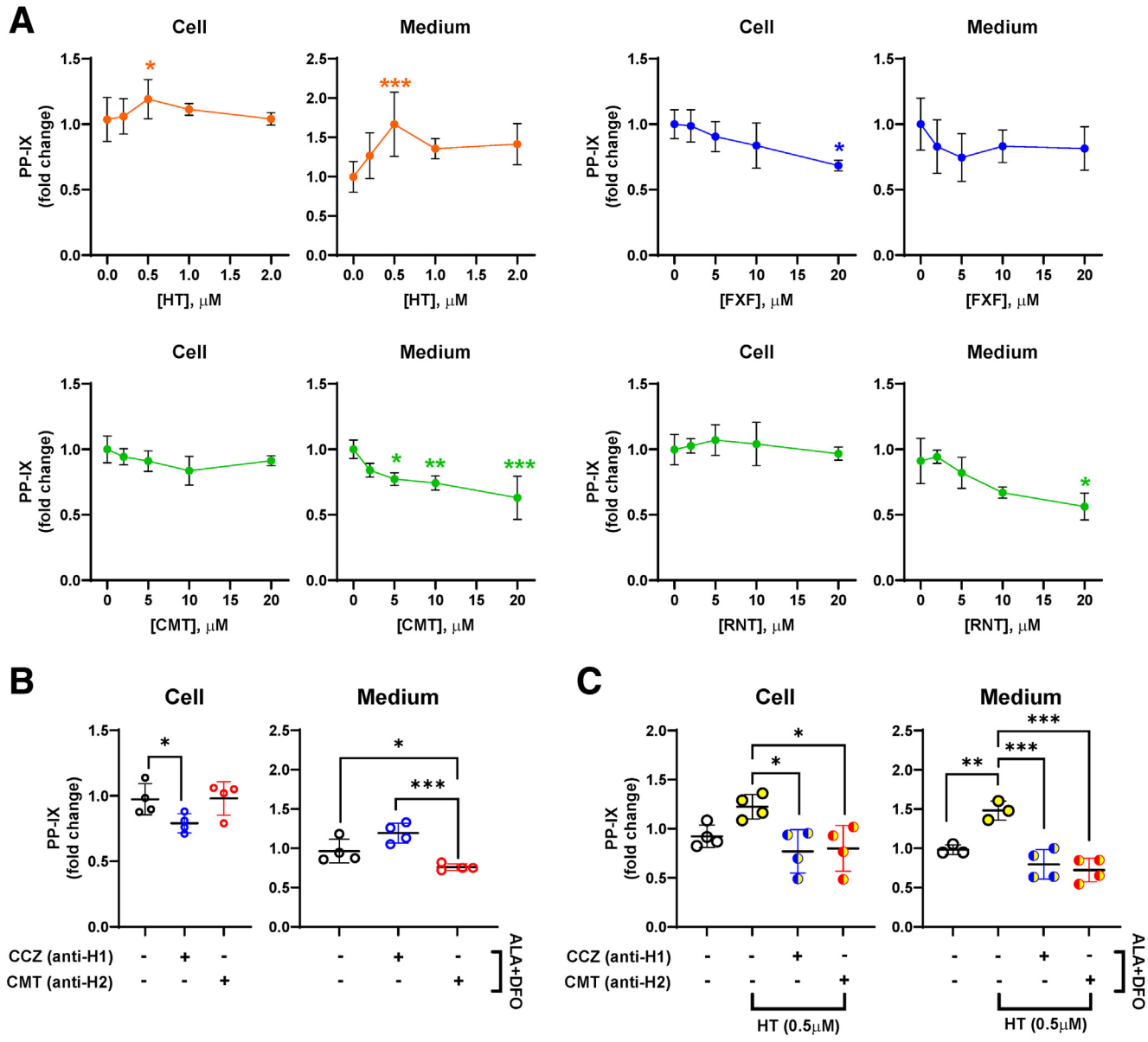

Figure 6. The role of the histamine pathway in porphyrin-stressed PMHs. Primary mouse hepatocytes (PMHs) were challenged with ALA + DFO that results in porphyrin accumulation, then treated with histamine (HT), CCZ, or other histamine blockers for 12 hours. (*A*) PMHs were treated with HT, the H1-blocker fexofenadine (FXF), and the H2-blockers cimetidine (CMT) and ranitidine (RNT) at the indicated doses. Intracellular and culture medium PP-IX levels following the treatments are shown. (*B*) CCZ and CMT were tested individually at 10 μM. Intracellular and medium PP-IX levels were measured in the absence of histamine. (*C*) CCZ and CMT were tested individually at 10 μM by treating primary mouse hepatocyte cultures. Intracellular and culture medium PP-IX levels in the presence or absence of histamine with levels relative to the condition without histamine. Data are shown as mean ± SD (n ≥3 experiments). Statistical analysis was performed by 1-way ANOVA test, ***$P < .001$; **$P < .01$; *$P < .05$.

study for histamine and its blockers using PMH challenged with ALA and DFO. Of the 4 histamine receptor subtypes, H1 and histamine receptor type 2 (H2) are expressed in the liver across multiple species including zebrafish,[16,17] mouse,[11,17] and human.[17–19] At 0.5 μM, histamine modestly increased PP-IX synthesis in hepatocytes by nearly 20% but greatly increased medium PP-IX by nearly 70% (Figure 6*A*). This stimulatory effect disappeared when it was given at higher doses, possibly due to cytotoxicity.

To complement our findings with CCZ, a first-generation H1-blocker, we tested fexofenadine, a second-generation H1-blocker, and the 2 acid-suppressor H2-blockers, cimetidine (CMT) and ranitidine. CMT is of particular interest because it has previously been described to inhibit ALA synthase-1[20] and is currently undergoing a phase II clinical trial for the treatment of human EPP (ClinicalTrial.gov: NCT05020184).[21] In our *in vitro* EPP model, fexofenadine reduced relative cell PP-IX level, and the H2 blockers CMT

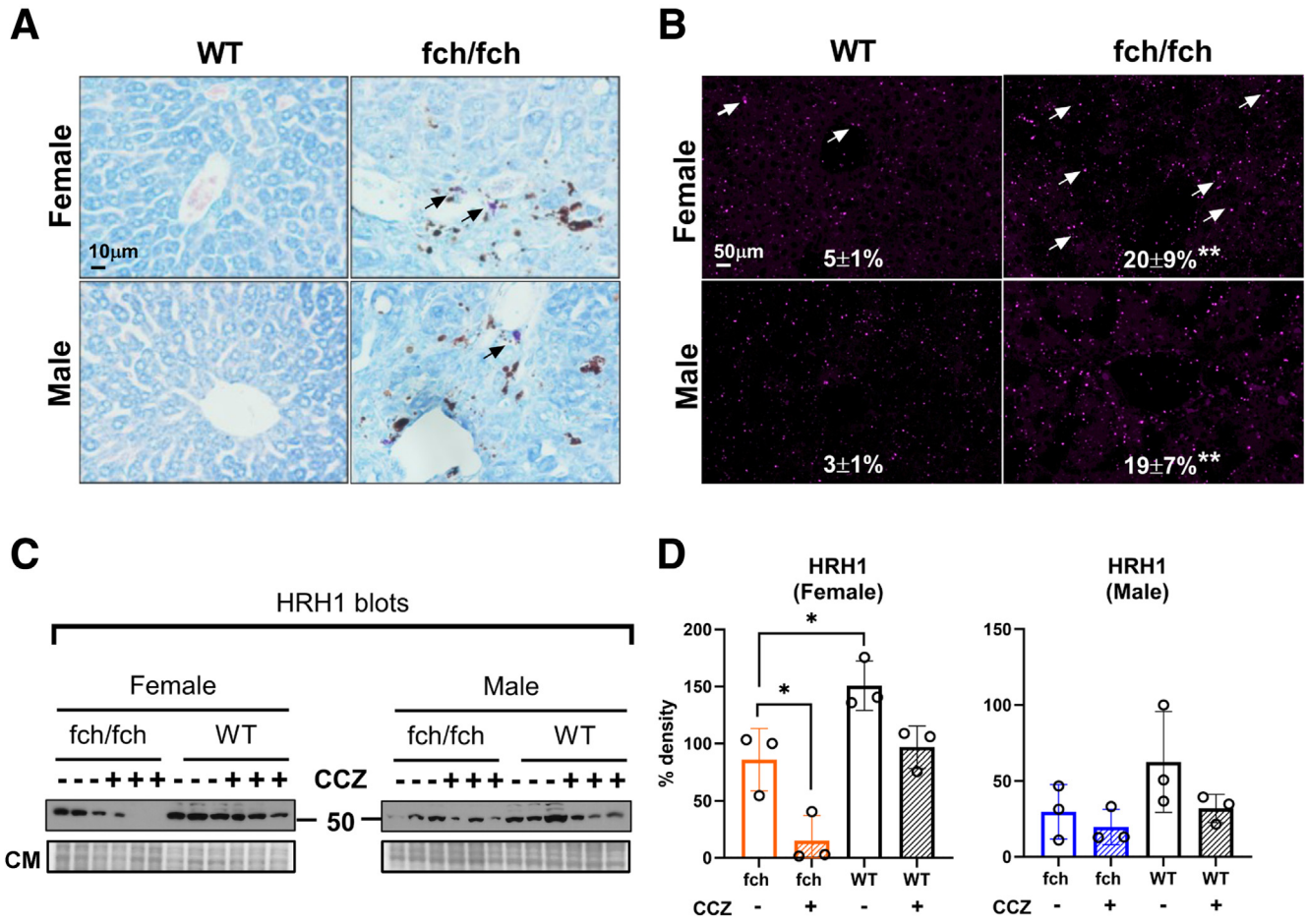

Figure 7. MC presence and HRH1 expression in wild-type and fch/fch livers. (*A*) May-Grunwald Giemsa staining of wild-type and fch/fch livers. Mast cell staining is highlighted by black arrows. (*B*) Immunofluorescence staining of MCP1 in wild-type (WT) and fch/fch livers (MCP1 puncta are indicated by *white arrows*) with quantified relative staining shown. The MCP1 staining images of the fch/fch (PBS) group in figures 7*B* (right panels) and 8*A* (first and third panels from left) were taken from a representative mouse liver section. Quantification is based on a group of immunofluorescence stainings (n = 3 livers, 2 image fields per liver). Another group (n = 2 livers, 2 images fields per liver) manifested a similar trend. (*C*) Immunoblots of the histamine receptor H1 (HRH1) in total liver lysates obtained from fch/fch and WT female and male mice with or without treatment with CCZ. (*D*) Densitometry analysis of HRH1 expression shown in panel *C*. HRH1 expression is suppressed in female fch/fch mice when compared with their WT controls, and CCZ further decreases HRH1 expression preferentially in female livers. Data are shown as mean ± SD (n = 3 livers/group). Statistical analysis was performed using the 1-way ANOVA test, $^*P < .05$.

and ranitidine lowered medium PP-IX levels but did not affect cell PP-IX levels (Figure 6*A*).

We then tested CCZ and CMT side by side in the presence and absence of histamine. Notably, CCZ reduced intracellular PP-IX by 20%, whereas CMT did not have a significant effect; conversely, CMT reduced medium PP-IX level by 24%, and CCZ did not show a significant effect (Figure 6*B*). However, when histamine was present, which increases intracellular PP-IX by 20%, both CCZ and CMT reversed the histamine effect and further decreased cell PP-IX by an additional 20% (Figure 6*C*). Similarly, histamine increased medium PP-IX levels by 50%, and this increase was inhibited by CCZ and CMT (Figure 6*C*). In summary, given that H1- and H2-blockade led to PP-IX reduction in different compartments (cell vs medium), it is likely that H1- and H2-antihistamines act on different signaling pathways.

CCZ Decreases MC Presence and Histamine Level in the fch/fch Liver and Plasma

Because MCs are a major source of histamine in the body, we evaluated their abundance in the liver using Giemsa staining and immunofluorescence staining of mast cell protease-1 (MCP1). Compared with wild-type livers, which show minimal Giemsa or MCP1 staining, both male and female fch/fch livers display heightened MC presence (Figure 7*A, B*). Baseline histamine receptor type 1 (HRH1) expression is reduced in female fch/fch livers when compared with wild-type livers, with CCZ administration leading to a further decrease in HRH1 expression in female livers (Figure 7*C, D*). Notably, CCZ treatment of fch/fch mice depleted MC in livers of both sexes (Figure 8*A*), but protein levels of MCP1 as determined by immunoblotting decreased more prominently in female livers (Figure 8*B*). Importantly,

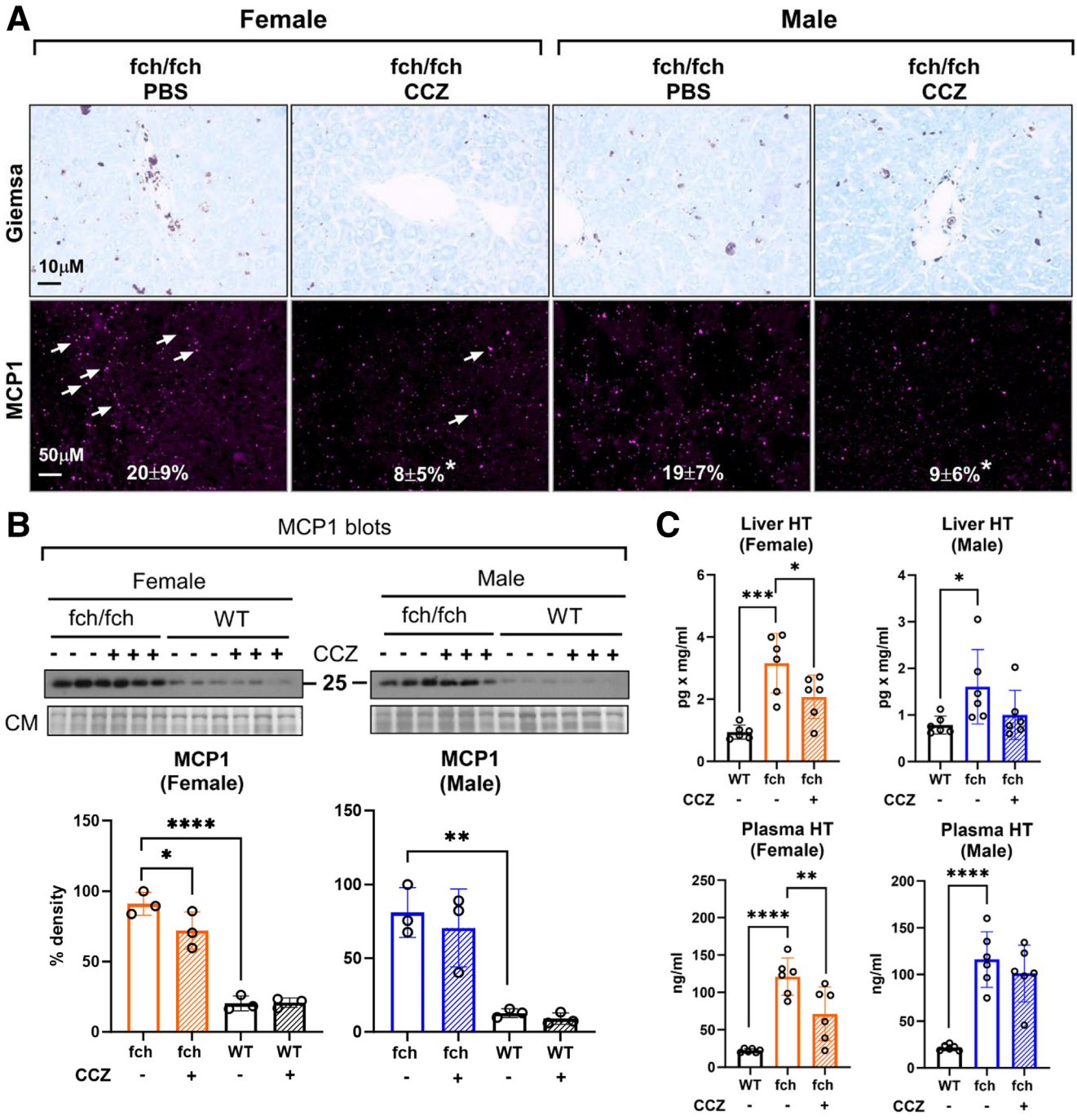

Figure 8. CCZ reduces MC presence and histamine levels in the female liver and plasma. (*A*) May-Grunwald Giemsa staining and immunofluorescence staining of mast cell protease 1 (MCP1) on fch/fch and wild-type livers. MCP1 puncta are indicated by *white arrows*. Expressions of MCP1 puncta are shown as mean percent cell area ± SD (n = 3 livers, 2 image fields/liver). (*B*) Immunoblot and densitometry analysis of MCP1 in fch/fch and wild-type livers (n = 3 livers/group). CM, Coomassie staining. (*C*) Histamine levels in the liver and plasma. Data are shown as mean ± SD (n = 6 mice/group). Statistical analysis was performed by 1-way ANOVA test, ****$P < .0001$; ***$P < .001$; **$P < .01$; *$P < .05$.

hepatic and plasma histamine levels increase dramatically in fch/fch mice (compared with wild-type controls), and this increase was reversed by CCZ only in the female mice (Figure 8*C*).

CCZ Transactivates Hepatic CAR and FXR in a Female-Selective Manner

Similar to what was reported in human EPP, in terms of a compensatory response to excess PP-IX production,[22]

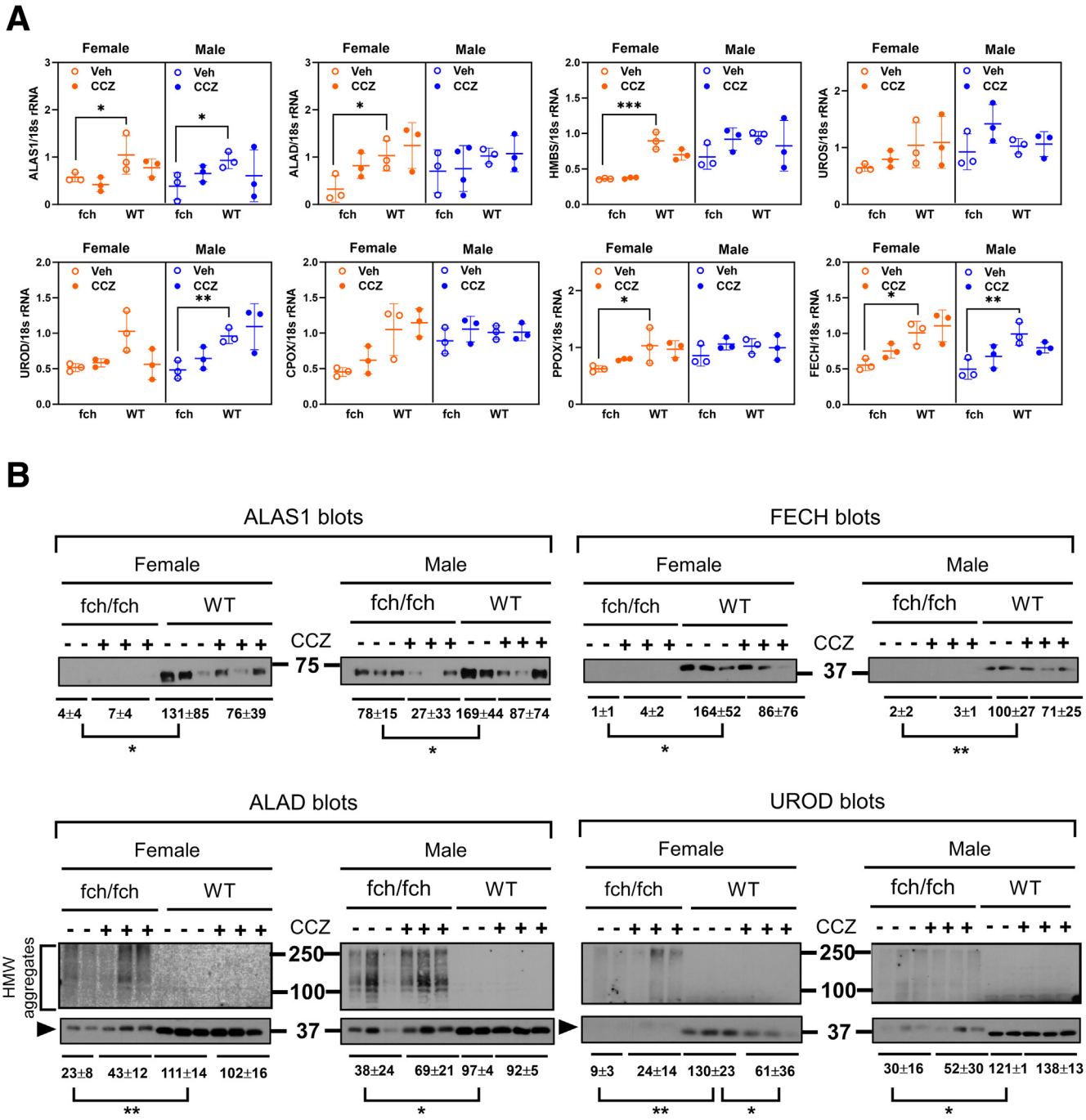

Figure 9. Gene mRNA and protein expressions of heme biosynthesis enzymes. (*A*) ALAS1, ALAD, HMBS, PPOX, and FECH gene expressions are suppressed in the female fch/fch liver. ALAS1, UROD, and FECH gene expressions are suppressed in the male fch/fch liver. (*B*) Standard immunoblotting was carried with similar protein loading for each of the displayed panels. The ALAS1, FECH, ALAD, and UROD protein expression is suppressed in the fch/fch livers. Under the experimental conditions used in this study, HMW aggregates of ALAD and UROD (and not ALAS1 or FECH) were detected in the fch/fch livers. There is an upward shift in ALAD and UROD monomers as indicated by the *arrowheads*. Data are shown as mean ± SD (n = 2–3 livers per group). Statistical analysis was performed by 1-way ANOVA test, ***$P < .001$; **$P < .01$; *$P < .05$.

mRNA expressions of all 8 heme biosynthetic enzymes in fch/fch mice of both sexes were either significantly suppressed or lower than the mean expression detected in wild-type mice (Figure 9*A*). This loss of expression was also reflected at the protein level (Figure 9*B*). CCZ did not alter the mRNA or protein expression of these enzymes, thereby suggesting that CCZ likely does not act on PP-IX biosynthesis.

To further pursue the possibility that CCZ enhances hepatic PP-IX clearance via excretion, we explored several key regulators in the liver that drive bile acid detoxification and

export. Constitutively active androstane receptor (CAR), the bile acid receptor farnesoid-X receptor (FXR), and their common transactivation partner retinoid X receptor (RXR) act in this capacity[23,24] (Figure 10*A*). Both CAR and FXR mRNA and protein were significantly suppressed in fch/fch livers, and CCZ further decreased their protein expressions in female

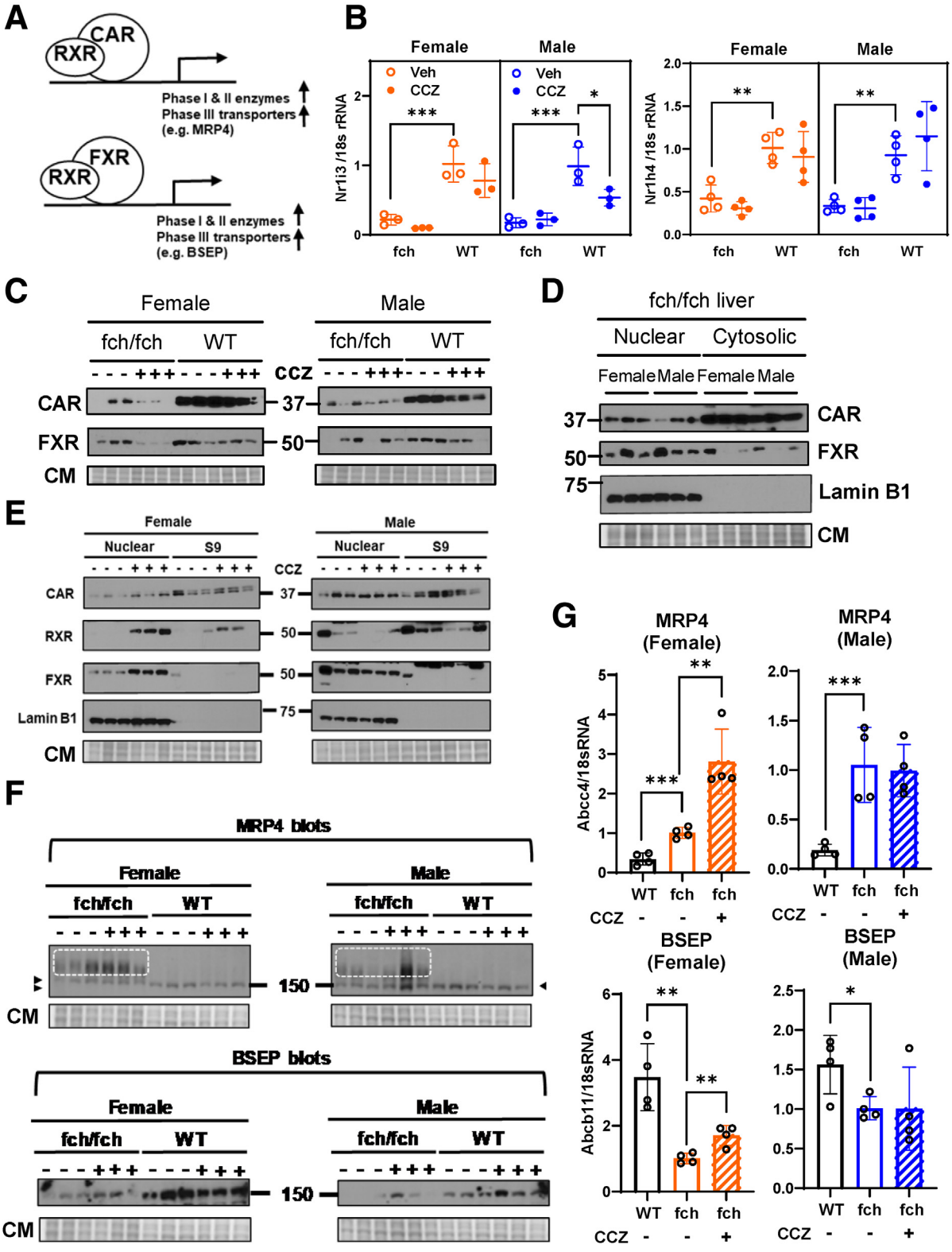

fch/fch livers (Figure 10*B, C*). Under basal conditions, CAR and FXR reside in the cytoplasm, and upon activation, both receptors enter the nucleus where they upregulate phase I and phase II detoxification enzymes and phase III transporters.[24,25] In fch/fch livers, a fraction of CAR and almost all FXR already translocate into the nuclear fraction (Figure 10*D*). Notably, CCZ treatment further enriches nuclear presence of CAR, FXR, and RXR, but this increased nuclear partitioning is observed only in female, and not male, mice (Figure 10*E*).

To verify that nuclear CAR and FXR induce elimination of PP-IX in bile by upregulating transporters, we examined MRP4 and BSEP, which are known respective targets of CAR[26,27] and FXR.[23,28] Hepatic MRP4 level is low but increases upon cholestasis, presumably as a defense mechanism to protect the liver from accumulation of cytotoxic bile acid.[27] In fch/fch livers, MRP4 was induced both at the mRNA and protein levels (Figure 10*F, G*). Although MRP4 protein was similarly upregulated in both sexes, MRP4 mRNA was further increased only in the female by CCZ. In the case of BSEP, both mRNA and protein were significantly suppressed in fch/fch livers, but CCZ reversibly upregulated its expression in females (Figure 10*F, G*). Immunofluorescence staining of MRP4 and BSEP also revealed a female-selective increase in their staining after CCZ treatment (Figure 11).

We also tested the effects of MRP4 and BSEP transporter knockdown in isolated PMHs (Figure 12). Transfection of small interfering RNAs (si-RNAs) and knockdown of MRP4 or BSEP were highly selective for the 2 transporters when compared with scrambled siRNA (Figure 12*A*), though it did not lead to a significant change in ALA + DFO-induced PP-IX accumulation in hepatocytes nor in the culture media (Figure 12*B*). However, knockdown of either MRP4 or BSEP led to a significant increase in the formation of p62 HMW aggregates as compared with scrambled siRNA (Figure 12*C, D*), thereby suggesting that the known PP-IX mediated protein oxidation via formation of reactive oxygen species (ROS), which leads to protein aggregation,[29] is enhanced when either MRP4 or BSEP level decreases. Under our study conditions, we observed protein aggregation in the absence of ALA + DFO (see lane 1 in Figure 12*A* for MRP4, and Figure 12*C* for p62), which was not seen in normal liver (see Figure 3*D* for p62 and Figure 10*F* for MRP4). We attribute this background aggregation to ROS generated by the lipofectamine transfection reagent.[30]

Discussion

Of the major therapeutics that had previously been attempted in the past 4 decades to treat EPP, only afamelanotide (Scenesse), an α-melanocyte-stimulating hormone analogue, received approval by the United States Food and Drug Administration in 2018.[31] This analogue was designed to target cutaneous EPP symptoms without addressing PP-IX accumulation in other organs. We performed a high-throughput drug screen using a porphyrin precursor administration in a zebrafish EPP model[8] and identified the H1-antihistamine CCZ as a highly effective PP-IX-lowering agent in zebrafish liver. This led us to examine and show that histamine promotes porphyrin accumulation and that H1 and H2-receptor blockade could be a viable strategy for treating EPP-related liver disease. Whether histamine receptor blockade also plays a role in skin manifestations remains to be determined.

CCZ and cimetidine are H1- and H2-antihistamines used to treat allergies and gastroduodenal ulcers, respectively.[32] They act as inverse agonists by binding to H1- or H2-histamine receptors and inhibit binding of histamine and subsequent Gαq/11 and Gαs signaling.[19,32] Upon surveying their safety profile, almost all H1/H2 antihistamines, with a few exceptions, are considered safe drugs for patients with porphyria based on recommendations provided by the American Porphyria Foundation (http://porphyriadrugs.com) and the Norwegian Porphyria Centre (https://www.drugs-porphyria.org/index.php) databases (Table 1). Although there is no reported safety data for CCZ in patients with porphyria, this first-generation antihistamine was approved in the 1940s and was reported to be a well-tolerated adjuvant antiviral agent for hepatitis C infection in human patients.[33]

PP-IX deposition has been noted in the severe cases of human EPP liver disease.[34,35] Here, we showed that histamine itself worsens PP-IX accumulation and increases its release from isolated mouse EPP hepatocytes (Figure 6*A, C*). The fch/fch mice also had elevated plasma histamine levels and heightened MC presence in the liver (Figure 7*B*). These findings suggest that histamine likely plays a pathologic role in driving PP-IX build-up and subsequent disease manifestation in the liver. Limited studies have reported that the oral H1 and H2 antihistamines terfenadine and cimetidine helped reduce skin photosensitivity in patients with EPP,[36–38] although the effect of histamine blockers on EPP-

Figure 10. (***See previous page***). **Expression and subcellular partitioning of CAR and FXR.** (*A*) Schematic diagram of the CAR/RXR and FXR/RXR gene transactivation system. (*B*) Relative mRNA expressions of Nr1i3/CAR and Nr1h4/FXR in female and male fch/fch vs wild-type (WT) livers (±CCZ). In WT male livers, CCZ treatment decreased CAR gene expression. (*C*) CAR and FXR protein expression is suppressed in fch/fch liver. CCZ administration decreases CAR and FXR protein expression further in livers of female fch/fch mice. (*D*) Liver homogenates were separated into nuclear- and cytoplasmic-enriched fractions. Baseline CAR and FXR expression is comparable in female and male fch/fch livers. Lamin B1 is used as a nuclear marker. Coomassie staining (CM) is included to show equal protein loading. (*E*) CCZ enriches nuclear localization of CAR, RXR, and FXR in female fch/fch livers. (*F*) Relative protein expression of MRP4 and BSEP. The MRP4 monomer is indicated by *arrowhead*. High molecular weight aggregates of MRP4 are highlighted by *white dotted boxes*. (*G*) Relative mRNA expression of MRP4 (*upper row*) and BSEP (*lower row*) in livers of female and male fch/fch (±CCZ) and WT mice. Statistical analysis was performed using the 1-way ANOVA test. ***$P < .001$; **$P < .01$; *$P < .05$.

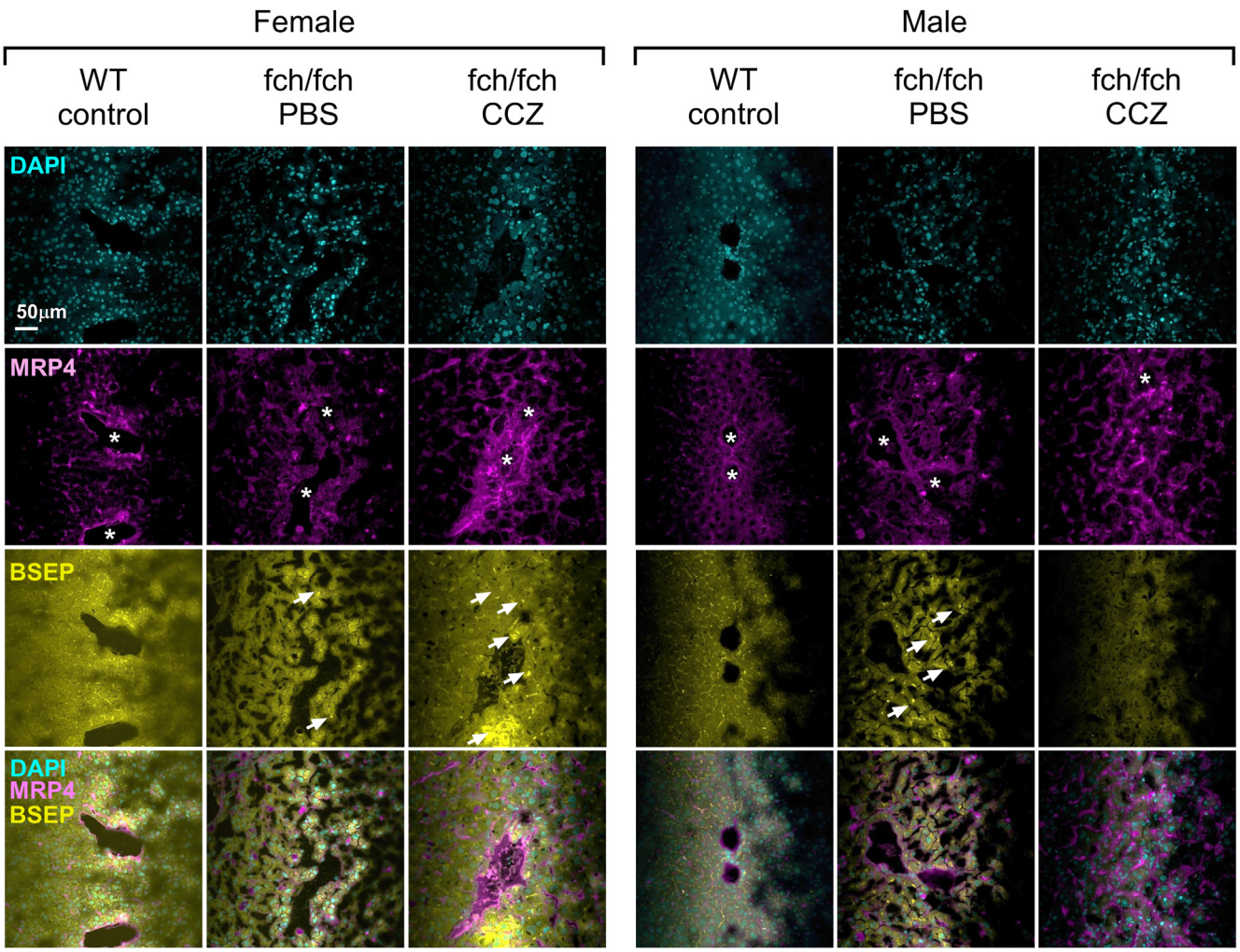

Figure 11. MRP4 and BSEP immunostaining in PBS- and CCZ-treated fch/fch livers. Representative images of liver sections stained with DAPI (to label nuclei) and anti-MRP4 and anti-BSEP antibodies. The MRP4 (*pink*) and BSEP (*yellow*) signal increases in the female livers following CCZ treatment. *Asterisks* indicate large bile ducts. *White arrows* indicate apical BSEP transporters that appear as *yellow lines*.

associated liver injury is unknown prior to the study herein. Notably, protein aggregation and oxidation are key drivers to porphyrin-mediated hepatocellular and liver tissue injury.[8,14,15,29,39] Our findings show that CCZ reduced protein aggregation and oxidation (Figure 3*D–F*) and ameliorated cellular and liver tissue injury (Figures 2,3, and 5). CCZ also decreased H1HR expression (Figure 7*C*), and together with other antihistamines, showed a PP-IX lowering effect in isolated mouse hepatocytes (Figure 2*D*). Therefore, antihistamines offer an attractive drug class to be examined in human EPP-related liver disease.

The enhanced excretion of toxic bile, and presumably the PP-IX admixed with it, has been a strategy explored in patients with EPP using bile acid sequestrants, cholestyramine, colestipol, and ursodeoxycholic acid.[40–42] Although reports of their clinical benefits were anecdotal, they provided proof-of-concept that enhanced bile excretion can ameliorate both cutaneous and hepatic EPP complications. Our findings showed that CCZ led to coordinated induction of the CAR/MRP4 and FXR/BSEP transactivation systems (Figure 10), and enhanced PP-IX excretion into the stool (Figure 3). Additionally, downregulation of MRP4 or BSEP led to increased protein aggregation of p62 (Figure 12). In support of our findings, MRP family members 5/9 have been described as heme exporters,[43–45] and a deleterious mutation in MRP9/ABCC12 causes cholestasis in zebrafish, mice, and humans.[46] Although the connection between the MRP family members, heme/porphyrin export, and cholestasis remains fragmentary and needs further investigation, our data suggests that MRP4, BSEP, or other MRPs may be potential molecular targets to enhance PP-IX clearance.

In both porphyria models we tested (fch/fch and DDC-fed mice), only females responded to CCZ treatment (Figures 3 and 5). This mouse female-selective phenotype was also noted at the molecular level, with CCZ enriching nuclear CAR and FXR accumulation in female but not male fch/fch livers. Sex-selective effects in CCZ metabolism have not been described in mice or humans, although it has been described in rats that CCZ is metabolized 8 times more efficiently in male vs female livers.[47] Because we only

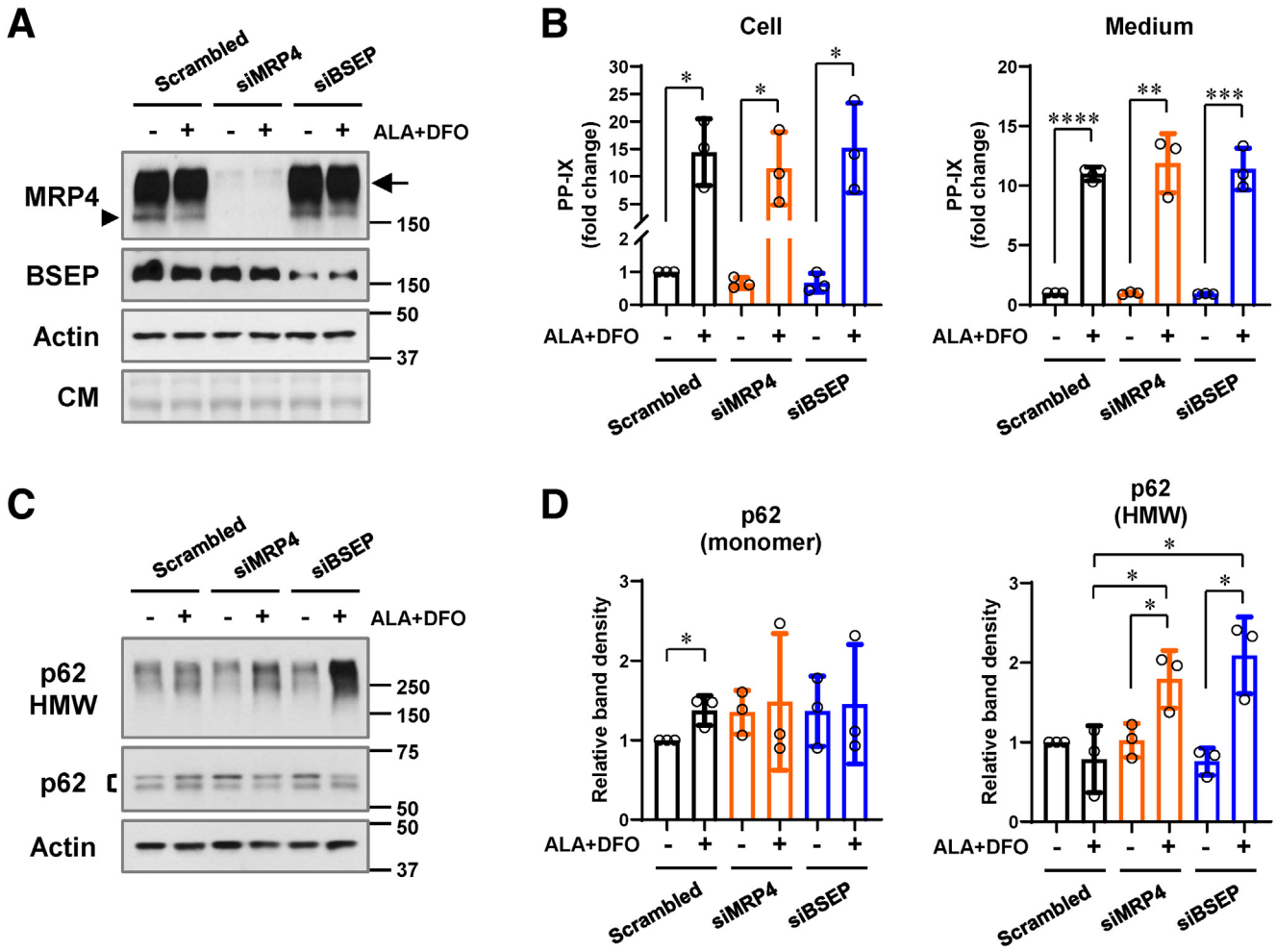

Figure 12. Effect of MRP4 and BSEP siRNA knockdown in ALA+DFO-treated PMH. (*A, B*) PMH were cultured with scrambled, MRP4, or BSEP siRNA (24 hours) followed by treatment with ALA + DFO (1 mM and 100 μM, respectively) for 12 hours. (*A*) Immunoblot analyses using antibodies to MRP4 and BSEP. Coomassie staining (CM) and actin blots are included to show equal loading. The MRP4 monomer is indicated by *arrowhead*. HMW aggregates of MRP4 are highlighted by an *arrow*. (*B*) Intracellular and culture medium PP-IX levels following the treatments are shown. (*C*) Immunoblots of p62 monomer doublet (detected as a doublet due to transfection conditions) and its HMW aggregates in total hepatocyte lysates. Actin blot is included as a loading control. (*D*) Relative densities of the p62 species from 3 individual experiments were quantified. For panels *B* and *D*, data are shown as mean ± SD (N = 3 experiments). Statistical analysis was performed by 2-tailed Student *t*-test, *****P* < .0001; ****P* < .001; ***P* < .01; **P* < .05.

observed protection in female fch/fch and DDC-fed mice, coupled with the previously reported male>female CCZ metabolism profile in rats, this suggests that it is the parent compound CCZ, and not its demethylated metabolite, norchlorcyclizine, that has the active porphyrin-lowering effect in female mice. We are not aware of similar metabolism differences in humans.

Furthermore, CCZ is reported to have potential drug-drug interactions, likely due to its effect on some cytochrome P-450 enzymes.[48] This provides a likely explanation for the observed ALT elevation in male but not female DDC-fed mice treated with CCZ (Figure 5*F*). Notably, the intraperitoneal dose of CCZ that we used in mice (25 mg/kg) converts to a human dose of 2 mg/kg,[49] which is likely compatible with safe dosing in humans of 50 mg oral tablet 2 to 4 times per day,[50] albeit plasma concentrations and half-maximal inhibitory concentration measurements would need to be carried out.

Two conceptual strategies to limit accumulation of toxic PP-IX involve inhibiting heme/porphyrin synthesis and/or clearing PP-IX through bile excretion. Our overall findings (Figure 13) present compelling evidence that the H1-antihistamine CCZ adopted both mechanisms whereby: (1) in the liver, it led to concerted induction of phase III transporters followed by increased bile/PP-IX excretion in zebrafish, isolated hepatocytes, and mouse models of EPP, and (2) systemically, CCZ decreases circulating and liver histamine levels, which in turn suppresses PP-IX biosynthesis. CCZ and cimetidine appear to have distinct effects that may relate to their noncanonical roles, which may differ for specific H1 or H2 blockers. Although cimetidine has been

Table 1. H1 Antihistamine Safety Recommendations for Patients With Porphyria

Chemical class	H1 antihistamines	APF	NAPOS
Piperazines	Cetirizine		
	Cyclizine		
	Levocetirizine		
Piperidines	Cyproheptadine		
	Desloratadine		
	Ebastine		
	Fexofenadine		
	Terfenadine		
Phenothiazines	Promethazine		
	Thiethylperazine		
Alkylamines	Chlorpheniramine		
Benzimidazole	Mizolastine		

Note: Data were accessed from the American Porphyria Foundation (APF) database and the Norwegian Porphyria Centre (NAPOS) database.
Note: Color key: dark green = safe; light green = probably safe; yellow = probably unsafe; red = unsafe.

described as an ALA synthase inhibitor,[20] recent findings suggest that this may not be the case,[51] although this may depend on the biologic context. Specifically, cimetidine is being investgated in a phase II clinical trial for its effect on photosensitivity in EPP.[21] It remains to be tested whether CCZ has an effect on skin manifestations of EPP, and whether its effect on bone marrow (Figure 3*A*) extends to other antihistamines. Through its dual ability to clear PP-IX and reduce protein aggregation and oxidation, CCZ or potentially other H1-blockers represent an attractive and likely safe drugs to be tested alone or in combination with cimetidine (or other H2-blockers) for patients with EPP who are at risk for developing hepatobiliary complications. In addition, X-linked protoporphyria (XLP) also leads to PP-IX accumulation due to a gain of function mutation in the enzyme 5'-aminolevulinate synthase-2 (ALAS2 or erythroid ALA-synthase) that is found in developing erythrocytes. Patients with XLP also develop photosensitivity and hepatobiliary disease. Therefore, the findings herein that relate to EPP may also extend to XLP, although this remains to be tested.[5,6]

Materials and Methods

Animals

All animal experiments were followed as approved by the Institutional Animal Care and Use Committee at Rutgers University and in accordance with the "Guide for the Care and Use of Laboratory Animals" published by the National Institutes of Health. Table 2 lists the commercial chemicals and reagents used in the study.

Chemical Libraries

The 2 compound libraries we used for our screening were the Prestwick Chemical Library (Prestwick Chemical) and the LOPAC (Sigma Aldrich). Each of the 2 libraries comprises 1280 compounds that were purposely selected to represent all the major drug classes. In the Prestwick

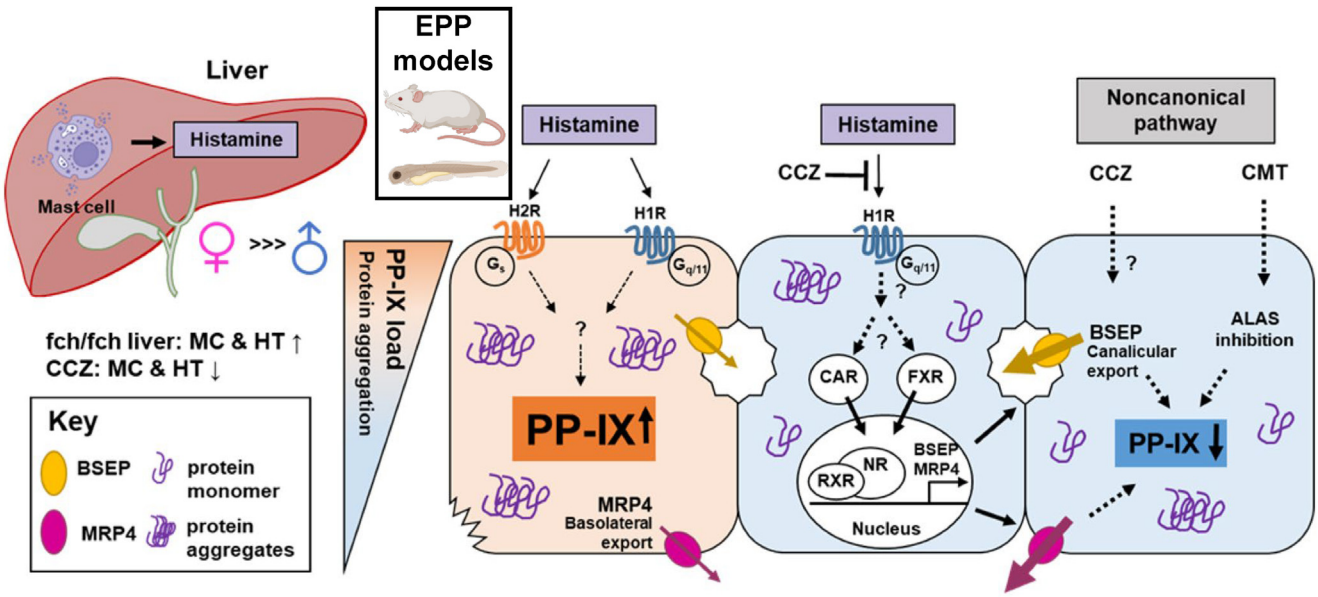

Figure 13. Schematic diagram of CCZ and histamine action in experimental EPP. In fch/fch liver, mast cell (MC) presence and histamine level increase. CCZ treatment depletes hepatic MC infiltrates and histamine levels. Histamine receptor types-1/2 (H1R/H2R) are expressed in human and mouse hepatocytes. When tested in porphyrin-stressed hepatocytes, histamine further increases intracellular PP-IX levels and induces protein aggregation (*left hepatocyte/orange*). Administration of H1R blocker CCZ or H2R blocker CMT reverses this effect, including inhibition of PP-IX-medicated protein aggregation (*right hepatocyte/blue*). CAR and FXR were found to translocate into the nucleus and transactivate bile acid transporters BSEP and MRP4 expression, leading to enhanced PP-IX excretion (*middle hepatocyte/blue*).

Table 2. Commercial Chemicals and Reagents Used in the Study

Reagents used in cell culture	Vendor	Catalog number
Protoporphyrin-IX	Enzo	ALX-430-041-G001
δ-aminolevulinic acid hydrochloride	Sigma Aldrich	A7793-1G
Deferoxamine mesylate salt	Sigma Aldrich	D9533-1G
Histamine ELISA kit	Abcam	ab213975

ELISA, enzyme-linked immunosorbent assay.

library, nearly 65% are approved by the United States Food and Drug Administration, and an additional 30% are approved by other agencies outside of the United States. For the LOPAC compounds, 25% are in the market, and the remaining 75% are bioactive molecules that have well-defined activities and a wide range of protein targets.

Primary Drug Screen in a Zebrafish EPP Model

Unbiased high-throughput drug screening was performed using an fabp10-fgb-egfp transgenic line of ABTL zebrafish (A3 line) that expresses the liver-specific protein fibrinogen-β, tagged with green fluorescent protein as previously described[52] and outlined in Figure 1.

At 6 days post-fertilization, the A3 larvae were retro-orbitally injected with 2 nanoliters of ALA hydrochloride (50 mg/mL) and DFO (50 mg/mL). Control larvae were injected with water (the control vehicle). Injected larvae were then incubated in E3 fish medium containing 4 Prestwick or LOPAC library compounds or the drug vehicle, dimethyl sulfoxide (DMSO). Each of the 8 384-well plates from the 2 libraries were multiplexed (4 compounds/well, each tested at 2 and 5 μM) into 96-well plates to maximize resources and time efficiency.

After injection, larvae were incubated in the dark for 24 hours before they were anesthetized and imaged with an Image Xpress Micro-imager (Molecular Devices) using 2 fluorescence readouts, fluorescein isothiocyanate (FITC) and Texas Red. The FITC channel was used to trace the green fluorescent livers. The traced livers were superimposed on the Texas Red channel, where the porphyrin signal was quantified. A positive hit was determined as a reduction in the red fluorescence porphyrin signal in the liver (Figure 1). Wells with a positive readout were subsequently deconvoluted to identify which of the 4 compounds in the positive wells accounted for the reduction. CCZ, which consistently and markedly reduced the red porphyrin signals, was selected for subsequent confirmation assays.

In Vitro EPP Model, Drug Treatment, and Porphyrin Measurement

Primary mouse hepatocytes were challenged with ALA + DFO (1 mM and 100 μM, respectively), which results in porphyrin accumulation, then treated with histamine, CCZ, or other histamine blockers. Cells were collected at indicated time points. Cell lysates and media porphyrins were prepared and measured as described.[15] In brief, the excitation wavelength was set at 400 nm, and the maxima PP-IX emission spectra was measured at 660 nm. A standard curve was generated using free acid PP-IX (Enzo). Cell lysates and culture media porphyrin levels were normalized to the protein content/sample and then expressed as ratio of the fluorescence unit detected from the untreated ALA + DFO group.

Primary Mouse Hepatocyte Isolation

Primary mouse hepatocytes were isolated from 8- to 10-week-old female FVB/N mice as described.[53] In brief, mice were anesthetized with 40 mg/kg pentobarbital (Vortech Pharmaceuticals, Ltd) before the livers were perfused with Hank's balanced salt solution containing 0.5 mM EGTA, 5.5 mM glucose, and 1% penicillin-streptomycin. Livers were then perfused with William's medium E (Gibco) and 40 U/L of collagenase IV (Worthington Biochemical Corporation). Liver parenchyma was then filtered through a 70-μM cell strainer (Fisher Scientific) and pelleted by centrifugation (50 *g*, 2 minutes, 4 °C). Cells were then seeded and allowed to attach for 6 hours before treatment.

In Vivo Efficacy Studies in Fech^{m1Pas} and DDC Mouse Model

Fech^{m1Pas} (fch/fch) mice (5–6 weeks old) were treated by intraperitoneal injection of CCZ (25 mg/kg) for 5 or 10 consecutive days. The CCZ dosing was selected after testing in a pilot experiment 10 mg/kg and 25 mg/kg dosing and observing that the 25 mg/kg is more effective in decreasing liver PP-IX levels (not shown). Also, the CCZ (25 mg/kg) dose we used is equivalent to a human dose of 2 mg/kg,[49] which is compatible with safe human dosing.[50] For the DDC model, 9-week-old BALB/c mice were fed with a regular chow diet containing 0.1% DDC and co-administered with CCZ (25 mg/kg, intraperitoneally) for 5 consecutive days. Liver, erythrocytes (cell pellet after removal of plasma), bone marrow, plasma, bile, and stool were collected for subsequent porphyrin quantification and fluorescence measurement. A subset of mice was single-housed in wired bottom cages where stools were collected every 48 hours. Parts of the livers were fixed with 10% formalin, stained with hematoxylin-eosin, then subjected to quantification of porphyrin deposits using Image J software. May-Grunwald Giemsa staining was performed to assess MC presence. Details related to sample preparation and porphyrin fluorescence measurement for each tissue are described.[15]

Gene Silencing With siRNA

Abcc4 (MRP4) siRNA and Abcb11 (BSEP) siRNA duplexes were obtained from Origene (Catalog#SR422676, Catalog#SR422664). Scrambled siRNA (Origene; Catalog#SR30004) was used as control. Transfections were conducted using the Lipofectamine RNAiMAX (Thermo Fisher Scientific) as recommended by the manufacturer.

Table 3. The RT-qPCR Primers Used in the Study

Transcript	Human (*Homo sapiens*) PCR primers	Mouse (*Mus musculus*) PCR primers
Alas1	ID: Hs.PT.56a.40544386.g 5′-ACATCACACAGCTCTTCCAG-3′ 5′- AAGTACATCTTCCGCCACAA-3′	ID: Mm.PT.58.7841429 5′-TGACTACCTAGGCATGAGTCG-3′ 5′-CTTGCTCGTTCCAGAAATATTCC-3′
Alad	ID: Hs.PT.56a.3971613 5′-AAGATCAAGACACAGCGTAGG-3′ 5′-AACCTCATCTACCCCATCTTTG-3′	ID: Mm.PT.58.29257918 5′-CCTCATCTATCCCATCTTTGTCA-3′ 5′-GGTCTCAGCATCTCTTCTAGC-3′
Hmbs	ID: Hs.PT.39a.22214823 5′-AGGGTACGAGGCTTTCAATG-3′ 5′-CATGTCTGGTAACGGCAATG-3′	ID: Mm.PT.39A.22214827 5′-AAAGATGAGGGTGATTCGAGTG-3′ 5′-AAGAATCTTGTCTCCCGTGG-3′
Uros	ID: Hs.PT.58.38508932 5′-TGTTCAGGTTCCCTTGGATTC-3′ 5′CCTGTGGAAACCTCAAAAGAGA-3′	ID: Mm.PT.58.13264122 5′-TGCCACCGCTTCTCTAGT-3′ 5′-TCTCCTTTGATAGTTCCACACG-3′
Urod	ID: Hs.PT.58.26811711 5′-GAGTGTAGTCTGTTTCCTCTCC-3′ 5′GATTGAGCTCGCAGTTACAGA-3′	ID: Mm.PT.58.31775813 5′-GTAGTTGGACTTGACTGGACAG-3′ 5′-CGACCGATCTCTTCCTCAGA-3′
Cpox	ID: Hs.PT.58.3495748 5′-TGAAGTACACAGCTGATGCC-3′ 5′GCGACATGAAGACCAAGATG-3′	ID: Mm.PT.58.41976009 5′-GTCCCTTCCTATGTTCCCATTG-3′ 5′-GCCCCGATCATACAACAGAT-3′
Ppox	ID: Hs.PT.58.21362284 5′-CAGTCATTAACAGCAACTCCCT-3′ 5′GTCCATCTACACAAGAACTGC-3′	ID: Mm.PT.58.42091252 5′-TCTTCACAATCACCTAGCAAGT-3′ 5′-CTTATAATGTGGTCAGCCTCCA-3′
Fech	ID: Hs.PT.58.25999059 5′-GTGAGCAGAAAACAGAATGACC-3′ 5′GTGGAGCACTATTGACAGGTG-3′	ID: Mm.PT.58.10646197 5′-CCATTGCTTTCACACAGTATCC-3′ 5′-GCCCACCTCGTTATAGTATCTG-3′
Nr1i3	N/A	ID: Mm.PT.58.13680704 5′-TGCTGATTCAGTTGCAAAGATG-3′ 5′-GCAGAAGTGTCTAAATGTTGGC-3′
Nr1h4	N/A	ID: Mm.PT.58.31148648 5′-TGAGCTGTGTGTTGTCTGTG-3′ 5′-GGCGTTCTTGGTAATGCTTC-3′
Abcb11	N/A	ID: Mm.PT.58.9240423 5′-GAAGTCCTCTCATCTATTCGAACA-3′ 5′-CACCATTCCTTTCCAAATTCCC-3′
Abcc4	N/A	ID: Mm.PT.58.41162071 5′-TGACTCACCAGTTACAGTACCT -3′ 5′-TTCAGAAAACTCCGTGTAAGTCC-3′

qRT-PCR, quantitative real-time polymerase chain reaction.

Quantitative Real-time Polymerase Chain Reaction

Total RNA was isolated (RNeasy mini kit, Qiagen) and purified according to manufacturer instructions. Quantitative real-time polymerase chain reaction was performed with an iQTM real-time PCR detection system (Bio-Rad) and SYBR green for monitoring cDNA amplification (Table 3 lists the primers used). Samples were analyzed in duplicates, and 5 individual mice were typically tested for each group. 18s RNA was used as an internal control, and transcript levels relative to 18s RNA were determined and reported as the mean ± standard deviation (SD).

Immunofluorescence Staining and Protein Analysis by Immunoblotting

Cells or livers were lysed in 2% SDS-containing sample buffer under reducing conditions. Nuclear and S9 (which consists of microsomes and cytosol) fractions were prepared in 1% NP40 buffer (4 °C) and isolated following centrifugation at 500*g* (4 °C, 10 minutes). Protein oxidative status was analyzed globally using the Protein Carbonyl Assay Kit (Abcam) as recommended by the manufacturer. For staining, liver sections were fixed in ice-cold methanol (20 minutes) then processed using standard procedures. Table 4 lists the antibodies used in the study. The MCP1 antibodies used were: for immunofluorescence staining from Thermo Fisher Scientific (catalog # 14-5503-82), and for immunoblotting from R&D Systems (catalog # AF5146).

Quantification of PP-IX Deposits in fch/fch and DDC-treated Mice

The liver PP-IX deposits were quantified using ImageJ software. After downloading the software, selected images were converted to grayscale (by selecting

Table 4. Commercial Antibodies Used in the Study

Category	Antibody	Vendor	Catalog number	Host species
Nuclear proteins	CAR/NR1I3	Novus Biologicals	N4111	Mouse
	FXR/NR1H4	Cell Signaling Technology	72105	Mouse
	RXRα/β/γ	Santa Cruz Biotechnology	sc-46659	Mouse
	LAMIN B1	Abcam	ab16048	Rabbit
Heme and porphyrin biosynthesis	ALAS-H	Santa Cruz Biotechnology	sc-137093	Mouse
	FECH		sc-377377	Mouse
	ALAD	Sigma-Aldrich	AV41657	Rabbit
	UROD	Proteintech	15547-1-AP	Rabbit
Bile acid transporters	BSEP/ ABCB11	Abcam	ab155421	Rabbit
	MRP4	Santa Cruz Biotechnology	sc-59614	Rat
Other proteins	p62/SQSTM1	Abcam	ab109012	Rabbit
	HRH1	ABclonal	A1422	Rabbit
	Actin	Invitrogen	MA5-11869	Mouse

BSEP, bile salt export pump; CAR, constitutive androstane receptor; FXR, farnesoid-X receptor; HRH1, histamine receptor type 1; MRP4, multidrug resistance-associated protein 4; RXR, retinoid X receptor.

Image → Type → 8-bit). The threshold is then adjusted by navigating to Image → Adjust → Threshold. The image is then duplicated followed by setting 2 thresholds: one for PP-IX deposits and one for open area (eg, ductal area or blank area without any cells) and applying the settings. The threshold settings were assessed using multiple images to ensure the setting reflects the PP-IX deposits or open area. Once a threshold range is determined, it is used for all images. Measurement parameters are set by selecting Analyze → Set Measurements and choosing options like Area and Integrated Density. Use Analyze Particles was applied to measure PP-IX deposits, adjusting the particle size (eg, 100 pixels) to exclude debris. After the analysis, the results were exported to Excel for further categorization, such as grouping PP-IX deposits by size. These steps were repeated for measuring open areas while keeping the default particle size settings. The PP-IX deposit area (%) = PP-IX area / (total area − open area).

Statistics

Statistical significance was assessed with GraphPad Prism 8.0 software. Data are presented as means ± SD ($n \geq 3$). The Student *t*-test or 1-way analysis of variance (ANOVA) was used to determine any statistically significant differences between the means of 2, 3, or more independent groups. Error bars represent standard deviation of the mean ($^{*}P < .05$; $^{**}P < .01$; $^{***}P < .001$; $^{****}P < .0001$).

References

1. Puy H, Gouya L, Deybach JC. Porphyrias. Lancet 2010; 375:924–937.
2. Bonkovsky HL, Guo JT, Hou W, et al. Porphyrin and heme metabolism and the porphyrias. Compr Physiol 2013;3:365–401.
3. Balwani M, Naik H, Anderson KE, et al. Clinical, biochemical, and genetic characterization of North American patients with erythropoietic protoporphyria and X-linked protoporphyria. JAMA Dermatol 2017; 153:789–796.
4. Wahlin S, Stal P, Adam R, et al; European Liver and Intestine Transplant Association. Liver transplantation for erythropoietic protoporphyria in Europe. Liver Transpl 2011;17:1021–1026.
5. Levy C, Dickey AK, Wang B, et al; Porphyrias Consortium of the Rare Diseases Clinical Network. Evidence-based consensus guidelines for the diagnosis and management of protoporphyria-related liver dysfunction in erythropoietic protoporphyria and X-linked protoporphyria. Hepatology 2024;79:731–743.
6. Heerfordt IM, Lerche CM, Philipsen PA, Wulf HC. Experimental and approved treatments for skin photosensitivity in individuals with erythropoietic protoporphyria or X-linked protoporphyria: a systematic review. Biomed Pharmacother 2023;158:114132.
7. Langendonk JG, Balwani M, Anderson KE, et al. Afamelanotide for erythropoietic protoporphyria. N Engl J Med 2015;373:48–59.
8. Elenbaas JS, Maitra D, Liu Y, et al. A precursor-inducible zebrafish model of acute protoporphyria with hepatic protein aggregation and multiorganelle stress. FASEB J 2016;30:1798–1810.
9. Tutois S, Montagutelli X, Da Silva V, et al. Erythropoietic protoporphyria in the house mouse. A recessive inherited ferrochelatase deficiency with anemia, photosensitivity, and liver disease. J Clin Invest 1991;88: 1730–1736.
10. Hanada S, Snider NT, Brunt EM, et al. Gender dimorphic formation of mouse Mallory-Denk bodies and the role of xenobiotic metabolism and oxidative stress. Gastroenterology 2010;138:1607–1617.
11. Kennedy L, Hargrove L, Demieville J, et al. Blocking H1/H2 histamine receptors inhibits damage/fibrosis in Mdr2(-/-) mice and human cholangiocarcinoma tumorigenesis. Hepatology 2018;68:1042–1056.
12. Pham L, Kennedy L, Baiocchi L, et al. Mast cells in liver disease progression: an update on current studies and implications. Hepatology 2022;75:213–218.

13. Bloomer JR. Liver metabolism of porphyrins and haem. J Gastroenterol Hepatol 1998;13:324–329.
14. Maitra D, Carter EL, Richardson R, et al. Oxygen and conformation dependent protein oxidation and aggregation by porphyrins in hepatocytes and light-exposed cells. Cell Mol Gastroenterol Hepatol 2019;8:659–682.e1.
15. Maitra D, Elenbaas JS, Whitesall SE, et al. Ambient light promotes selective subcellular proteotoxicity after endogenous and exogenous porphyrinogenic stress. J Biol Chem 2015;290:23711–23724.
16. Peitsaro N, Sundvik M, Anichtchik OV, et al. Identification of zebrafish histamine H1, H2 and H3 receptors and effects of histaminergic ligands on behavior. Biochem Pharmacol 2007;73:1205–1214.
17. Wang M, Wei X, Shi L, et al. Integrative genomic analyses of the histamine H1 receptor and its role in cancer prediction. Int J Mol Med 2014;33:1019–1026.
18. Akdis CA, Simons FE. Histamine receptors are hot in immunopharmacology. Eur J Pharmacol 2006;533:69–76.
19. Thangam EB, Jemima EA, Singh H, et al. The role of histamine and histamine receptors in mast cell-mediated allergy and inflammation: the hunt for new therapeutic targets. Front Immunol 2018;9:1873.
20. Marcus DL, Halbrecht JL, Bourque AL, et al. Effect of cimetidine on delta-aminolevulinic acid synthase and microsomal heme oxygenase in rat liver. Biochem Pharmacol 1984;33:2005–2008.
21. Leaf RK, Dickey AK. How I treat erythropoietic protoporphyria and X-linked protoporphyria. Blood 2023; 24:2921–2931.
22. Bloomer J, Wang Y, Singhal A, et al. Molecular studies of liver disease in erythropoietic protoporphyria. J Clin Gastroenterol 2005;39(4 Suppl 2):S167–S175.
23. Kakizaki S, Takizawa D, Tojima H, et al. Xenobiotic-sensing nuclear receptors CAR and PXR as drug targets in cholestatic liver disease. Curr Drug Targets 2009;10:1156–1163.
24. Yang H, Wang H. Signaling control of the constitutive androstane receptor (CAR). Protein Cell 2014;5:113–123.
25. Halilbasic E, Claudel T, Trauner M. Bile acid transporters and regulatory nuclear receptors in the liver and beyond. J Hepatol 2013;58:155–168.
26. Chai J, Luo D, Wu X, et al. Changes of organic anion transporter MRP4 and related nuclear receptors in human obstructive cholestasis. J Gastrointest Surg 2011; 15:996–1004.
27. Assem M, Schuetz EG, Leggas M, et al. Interactions between hepatic Mrp4 and Sult2a as revealed by the constitutive androstane receptor and Mrp4 knockout mice. J Biol Chem 2004;279:22250–22257.
28. Plass JR, Mol O, Heegsma J, et al. Farnesoid X receptor and bile salts are involved in transcriptional regulation of the gene encoding the human bile salt export pump. Hepatology 2002;35:589–596.
29. Maitra D, Bragazzi Cunha J, Elenbaas JS, et al. Porphyrin-induced protein oxidation and aggregation as a mechanism of porphyria-associated cell injury. Cell Mol Gastroenterol Hepatol 2019;8:535–548.
30. Kongkaneramit L, Sarisuta N, Azad N, et al. Dependence of reactive oxygen species and FLICE inhibitory protein on lipofectamine-induced apoptosis in human lung epithelial cells. J Pharmacol Exp Ther 2008;325:969–977.
31. Ratner M. Patients with porphyria bask in sunlight of FDA approval. Nat Biotechnol 2019;37:1390–1391.
32. Simons FE, Simons KJ. Histamine and H1-antihistamines: celebrating a century of progress. J Allergy Clin Immunol 2011;128:1139–1150.e4.
33. Koh C, Dubey P, Han MAT, et al. A randomized, proof-of-concept clinical trial on repurposing chlorcyclizine for the treatment of chronic hepatitis C. Antiviral Res 2019; 163:149–155.
34. Bloomer JR, Phillips MJ, Davidson DL, et al. Hepatic disease in erythropoietic protoporphyria. Am J Med 1975;58:869–882.
35. McGuire BM, Bonkovsky HL, Carithers RL Jr, et al. Liver transplantation for erythropoietic protoporphyria liver disease. Liver Transpl 2005;11:1590–1596.
36. Farr PM, Diffey BL, Matthews JN. Inhibition of photosensitivity in erythropoietic protoporphyria with terfenadine. Br J Dermatol 1990;122:809–815.
37. Yamamoto S, Hirano Y, Horie Y. Cimetidine reduces erythrocyte protoporphyrin in erythropoietic protoporphyria. Am J Gastroenterol 1993;88:1465–1466.
38. Tu JH, Sheu SL, Teng JM. Novel treatment using cimetidine for erythropoietic protoporphyria in children. JAMA Dermatol 2016;152:1258–1261.
39. Maitra D, Pinsky BM, Soherawardy A, et al. Protein-aggregating ability of different protoporphyrin-IX nanostructures is dependent on their oxidation and protein-binding capacity. J Biol Chem 2021;297:100778.
40. McCullough AJ, Barron D, Mullen KD, et al. Fecal protoporphyrin excretion in erythropoietic protoporphyria: effect of cholestyramine and bile acid feeding. Gastroenterology 1988;94:177–181.
41. Tishler PV, Rosner B. Treatment of erythropoietic protoporphyria with the oral sorbent colestipol: a proof-of-concept clinical trial. J Am Acad Dermatol 2014;70:391–392.
42. Fujimori N, Komatsu M, Tanaka N, et al. Cimetidine/lactulose therapy ameliorates erythropoietic protoporphyria-related liver injury. Clin J Gastroenterol 2017;10:452–458.
43. Korolnek T, Zhang J, Beardsley S, et al. Control of metazoan heme homeostasis by a conserved multidrug resistance protein. Cell Metab 2014;19:1008–1019.
44. Chambers IG, Kumar P, Lichtenberg J, et al. MRP5 and MRP9 play a concerted role in male reproduction and mitochondrial function. Proc Natl Acad Sci U S A 2022; 119:e2111617119.
45. Wang Z, Zeng P, Zhou B. Identification and characterization of a heme exporter from the MRP family in Drosophila melanogaster. BMC Biol 2022;20:126.
46. Pham DH, Kudira R, Xu L, et al. Deleterious variants in ABCC12 are detected in idiopathic chronic cholestasis and cause intrahepatic bile duct loss in model organisms. Gastroenterology 2021;161:287–300.e16.
47. Kuntzman R, Klutch A, Tsai I, et al. Physiological distribution and metabolic inactivation of chlorcyclizine and cyclizine. J Pharmacol Exp Ther 1965;149:29–35.
48. Bonfils C, Dalet C, Dalet-Beluche I, Maurel P. Cytochrome P-450 isozyme LM3b from rabbit liver

microsomes. Induction by triacetyloleandomycin purification and characterization. J Biol Chem 1983; 258:5358–5362.
49. Nair AB, Jacob S. A simple practice guide for dose conversion between animals and human. J Basic Clin Pharm 2016;7:27–31.
50. Schafer A, Cheng H, Xiong R, et al. Repurposing potential of 1st generation H1-specific antihistamines as anti-filovirus therapeutics. Antiviral Res 2018;157:47–56.
51. Yasuda M, Lee S, Gan L, et al. Cimetidine does not inhibit 5-aminolevulinic acid synthase or heme oxygenase activity: Implications for treatment of acute intermittent porphyria and erythropoietic protoporphyria. Biomolecules 2023;14:27.
52. Vo AH, Swaroop A, Liu Y, et al. Loss of fibrinogen in zebrafish results in symptoms consistent with human hypofibrinogenemia. PLoS One 2013;8:e74682.
53. Weerasinghe SV, Park MJ, Portney DA, Omary MB. Mouse genetic background contributes to hepatocyte susceptibility to Fas-mediated apoptosis. Mol Biol Cell 2016;27:3005–3012.

Received September 15, 2024. Accepted January 8, 2025.

Correspondence
Address correspondence to: Bishr Omary, MD, PhD, Center for Advanced Biotechnology and Medicine, Rutgers University. 679 Hoes Lane West, Piscataway, New Jersey. e-mail: bishr.omary@rutgers.edu.

Acknowledgments
The authors thank the Center for Chemical Genomics, and the Advanced Genomics Core at the University of Michigan for technical assistance with the initial drug screening.

CRediT Authorship Contributions

Ning Kuo (Conceptualization: Supporting; Data curation: Lead; Formal analysis: Equal; Investigation: Lead; Methodology: Lead; Software: Lead; Validation: Lead; Visualization: Lead; Writing – original draft: Lead)

Pei Li, PhD, MD (Data curation: Supporting; Formal analysis: Supporting; Investigation: Supporting; Validation: Supporting; Visualization: Supporting)

Juliana Bragazzi Cunha, PhD (Data curation: Supporting; Formal analysis: Supporting; Investigation: Supporting; Methodology: Supporting; Visualization: Supporting)

Lu Chen (Investigation: Supporting)

Jordan A. Shavit (Funding acquisition: Supporting; Investigation: Supporting; Methodology: Supporting; Resources: Supporting)

Bishr Omary, PhD, MD (Conceptualization: Lead; Data curation: Supporting; Formal analysis: Equal; Funding acquisition: Lead; Investigation: Supporting; Methodology: Supporting; Project administration: Lead; Resources: Lead; Supervision: Lead; Validation: Supporting; Writing – review & editing: Lead)

Conflicts of interest
These authors disclose the following: Bishr Omary serves (2021 to present) as member of the National Institutes of Health (NIH)/National Institute of Diabetes and Digestive and Kidney Diseases Data and Safety Monitoring Board of the NIH-supported Porphyrias Consortium (PC). The PC includes Herbert Bonkovsky, who is an unpaid consultant of an NIH R01 (DK116548; PI, Bishr Omary), and has collaborated with some of the authors on 3 publications (2011, 2015, 2021). None of the PC members are involved with this study. A provisional patent application has been submitted for the use of anti-histamine H1-receptor blockers with or without anti-histamine H2-receptor blockers to treat protoporphyrias that associate with protoporphyrin-IX accumulation. The remaining authors disclose no conflicts.

Funding
This work is supported by National Institutes of Health grants R01 DK116548 (Bishr Omary), and R35 HL150784 and the Henry and Mala Dorfman Family Professorship of Pediatric Hematology/Oncology (Jordan Shavit).